Rocking response of rigid blocks under near-source ground motions

Article *in* Géotechnique · January 2000

DOI: 10.1680/geot.2000.50.3.243

2 authors, including:

Nicos Makris
Southern Methodist University
243 PUBLICATIONS **6,004** CITATIONS

SEE PROFILE

Makris, M. & Roussos, Y. (2000). *Géotechnique* **50**, No. 3, 243–262

Rocking response of rigid blocks under near-source ground motions

N. MAKRIS* and Y. S. ROUSSOS*

In this paper the transient rocking response of a rigid block subjected to trigonometric pulses and near-source ground motions is investigated in detail. First, the rocking response to a half-sine pulse motion is revisited. It is shown that the solution presented by Housner for the minimum acceleration amplitude of a half-sine pulse that is needed to overturn a rigid block is incorrect. In reality, under a half-sine pulse, a block overturns during its free vibration regime and not at the instant that the pulse expires, as was assumed by Housner. Within the limits of the linear approximation, the correct conditions for a block to overturn are established and the correct expression that yields the minimum acceleration required to overturn a block is derived. Subsequently, physically realizable cycloidal pulses are introduced and their resemblance to recorded near-source ground motions is illustrated. The study uncovers the coherent component of some near-source acceleration records, and the overturning potential of these motions is examined. It is found that the toppling of smaller blocks is more sensitive to the peak ground acceleration, whereas the toppling of larger blocks depends mostly on the incremental ground velocity. The kinematic characteristics of recorded near-source ground motions are examined in detail, and it is found that the high-frequency fluctuations that occasionally override the long-duration pulse will overturn a smaller block, whereas a larger block will overturn due to the long-duration pulse. A simple, yet dependable, method to determine the level of a recorded ground motion that is needed to overturn a given block is developed and illustrated through examples. The method examines the acceleration amplitude, and the duration and the type of distinct local pulses that are identifiable within the record, including the pulse that contains the peak ground acceleration. According to the type of each pulse identified, the method estimates the minimum acceleration amplitude needed to overturn a given block, and this value is compared with the recorded acceleration amplitude of each pulse identified within the record. In this light, the rocking response of rigid blocks subjected to strong near-source ground motions is shown to be quite ordered and predictable.

KEYWORDS: dynamics; rocking; overturning; near-source; earthquakes.

Dans la présente communication, on examine en détail la réponse oscillant transitoire d'un bloc rigide soumis à des impulsions trigonométriques et des mouvements du sol proches de la source. En premier lieu, on réexamine la réaction oscillant à un mouvement pulsatoire demi-sinusoïde. On démontre que la solution présentée par Housner pour l'amplitude à accélération minimum d'une impulsion demi-sinusoïde, nécessaire pour renverser un bloc rigide est erronée. En réalité, sous une impulsion à demi-sinusoïde, un bloc se renverse au cours de son régime de vibration libre et non pas au moment de l'expiration de l'impulsion, comme l'avait supposé Housner. Dans les limites de l'approximation linéaire, on établit les conditions correctes pour le renversement d'un bloc et on dérive l'expression précise donnant l'accélération minimale nécessaire d'un bloc et on dérive l'expression précise donnant l'accélération minimale nécessaire pour renverser un bloc. Ensuite, on introduit des impulsions cycloïdales réalisables physiquement et on illustre leur ressemblance avec des mouvements du sol enregistrés à proximité de la source. L'étude révèle l'élément cohérent de certains dossiers d'accélération à proximité de la source et examine le potentiel de renversement de ces mouvements. On s'est aperçu que le basculement de blocs de petite taille est plus sensible à l'accélération de pointe au sol, alors que le basculement de blocs de grande taille est en grande partie fonction de la vitesse incrémentale au sol. En examinant en détail les caractéristiques cinématiques de mouvements du sol enregistrés à proximité de leur source, on s'aperçoit que les fluctuations haute fréquence qui asservissent parfois l'impulsion de longue durée parviennent à renverser un bloc de petite taille, alors que l'inversion d'un bloc de grande taille se produit à la suite d'une impulsion de longue durée. On développe et on illustre une méthode à la fois simple et fiable pour déterminer le niveau de mouvement enregistré du sol nécessaire pour renverser un certain block et on l'illustre avec des exemples. Cette méthode examine l'amplitude de l'accélération, la durée et le type d'impulsions locales distinctes identifiables au sein de l'enregistrement, y compris l'impulsion contenant l'accélération de point au sol. En fonction du type de chacune des impulsions identifiées, la méthode estime l'amplitude d'accélération minimum nécessaire pour renverser un certain bloc, et cette valeur est comparée à l'amplitude d'accélération enregistrée de chaque impulsion identifiée dans l'enregistrement. Dans cette optique, on démontre que la réponse oscillante de la soumission de blocs rigides à de forts mouvements du sol à proximité de la source est très ordonnée et prévisible.

INTRODUCTION

During strong ground shaking, a variety of rigid structures, such as concrete radiation shields, electrical transformers and other heavy equipment, might slide or set into rocking motion that results in substantial damage. Early studies on the dynamic response of a rigid block supported on a base undergoing horizontal motion were presented by Housner (1963). In that study, the base acceleration was represented by a rectangular or a half-sine pulse, and expressions were derived for the minimum acceleration required to overturn the block. Using an energy approach, Housner presented an approximate analysis of the dynamics of a rigid block subjected to a white noise excitation and uncovered a scale effect that explained why the larger of two geometrically similar blocks can survive the excitation, whereas the smaller block may topple. He also indicated that toppling of a given block depends on the product of the acceleration amplitude of the pulse and its duration. This fundamental finding by Housner (1963), that toppling of a block depends on the incremental velocity (area under the acceleration pulse) and not merely on the peak ground acceleration (West's formula) (Milne, 1885; Hogan, 1989), did not receive the attention it deserved. Yim *et al.* (1980) adopted a probabilistic approach and conducted a numerical study using artificially generated ground motions to show that the rocking response of

Manuscript received 27 October 1997; revised manuscript accepted 8 October 1999.
Discussion on this paper closes 26 September 2000; for further details see p. ii.
* University of California, Berkley.

a block is sensitive to system parameters. Their simulation procedure consisted of generating samples of Gaussian white noise that was multiplied by an intensity function of time and subsequently filtered through a second-order linear filter to impart a smooth transfer function with a maximum at 2·5 Hz. The white-noise-type motions used by Yim *et al.* (1980) do not contain any coherent component, and the overturning of a block is the result of a rapid succession of small, random impulses. It is partly because of this very nature of ground motions used that the results of Yim *et al.* (1980) exhibit such a high sensitivity to system parameters.

Experimental and analytical studies on the same problem have been reported by Aslam *et al.* (1980). Their study concludes that, in general, the rocking response of blocks subjected to earthquake motion is in line with the conclusions derived from single pulse excitations; however, when artificially generated motions were used, the rocking response showed high sensitivity to the system parameters.

The rocking response of blocks subjected to harmonic steady-state loading was studied in detail by Spanos & Koh (1984), who identified 'safe' and 'unsafe' regions and developed analytical methods for determining the fundamental and subharmonic modes of the system. Their study was extended by Hogan (1989, 1990), who further elucidated the mathematical structure of the problem by introducing the concepts of orbital stability and Poincaré section. Hogan (1989) showed that there is a minimum value of the forcing amplitude, dependent on frequency, below which the block asymptotic motion ceases. Perhaps Hogan's (1989) most relevant finding for earthquake engineering is that the domain of maximum transients of his solutions appears to be relatively ordered, and possesses a high degree of predictability despite the unpredictability that is present in the asymptotic part of the solutions. The steady-state rocking response of rigid blocks was also studied analytically and experimentally by Tso & Wong (1989a,b). While their theoretical study was not as deep as the one presented by Hogan (1989), their experimental work provided valuable support to theoretical findings. Other related studies are referenced in the above-mentioned papers.

While the early work of Yim *et al.* (1980) used artificially generated white-noise-type motions, and the work of Spanos & Koh (1984), Hogan (1989, 1990) and Tso & Wong (1989a,b) used long-duration harmonic motions, our attention in this paper is redirected to pulse-type motions, which are found to be good representations of near-source ground motions (Campillo *et al.*, 1989; Iwan & Chen, 1994).

During a seismic event, the ground movement in the near-fault region is primarily the result of waves that are moving in the same direction as the fault rupture, thereby being crowded together to produce a long-duration pulse. In many cases, acceleration records contain high spikes and resemble the traditional random-like motions; however, their velocity and displacement histories uncover a coherent long-period pulse with some high-frequency fluctuations that override it. In this paper, we concentrate on the rocking response of rigid blocks subjected to near-source ground motions. We have built on Housner's (1963) pioneering work to show that a smaller block might overturn due to the high-frequency fluctuations that override the long-duration pulse, whereas a larger block will overturn due to the long-duration pulse.

We start our analysis by revisiting the rocking response of a rigid block subjected to a half-sine pulse. It is shown analytically that the solution presented by Housner (1963) for the minimum overturning acceleration amplitude is incorrect. This is because under a half-sine pulse a block overturns during its free vibration response and not at the instant that the pulse expires. Within the limits of the linear approximation, the correct conditions for a block to overturn are established and the correct expression that yields the minimum acceleration to overturn a block is derived.

Selected near-source ground motions are presented, and their resemblance to physically realizable cycloidal pulses is shown. A type A cycloidal pulse approximates to a forward pulse, a type B cycloidal pulse approximates to a forward-and-back pulse, whereas a type C_n pulse approximates a recorded motion that exhibits n main cycles in its displacement history. The velocity histories of all type A, type B and type C_n pulses are differentiable signals that result in finite acceleration values. Subsequently, the rocking response of a free standing block subjected to type A, type B and type C_n pulses is investigated. It is shown that the toppling of smaller blocks is more sensitive to the peak ground acceleration, whereas the toppling of larger blocks depends mostly on the incremental ground velocity, which is the net increment of the ground velocity along a monotonic segment of its time history. In the last section, the rocking response of free-standing blocks subjected to near-source ground motions is examined in detail. First, the effects of the non-linear nature of the rocking motion are illustrated and the accuracy of the non-linear numerical algorithm is validated. The simple approximate expressions derived to compute the minimum acceleration amplitude of a pulse that is needed to overturn a given block are used to predict the toppling of blocks. It is shown that blocks which are small enough for their frequency ratio to be below a cut-off frequency overturn due to high-acceleration, short-duration pulses, whereas blocks whose frequency ratio is above the cut-off frequency overturn due to longer-duration pulses with smaller acceleration. Finally, a simple method that involves hand calculations is developed to compute the cut-off frequency and the level of a recorded motion that is needed to overturn a given block.

PROBLEM DEFINITION AND EQUATIONS OF MOTION

We consider the model shown in Fig. 1, which can oscillate about the centres of rotation O and O′ when it is set to rocking. Its centre of gravity coincides with the geometric centre that is at a distance R from any corner. The angle α of the block is given by $\tan(\alpha) = b/h$. Depending on the value of the ground acceleration and the coefficient of friction, μ, the block may translate with the ground, or enter a rocking motion or a sliding motion. A necessary condition for the block to enter a rocking motion is $\mu > b/h$ (Aslam *et al.*, 1980; Scalia & Sumbatyan, 1996). The possibility of a block sliding during the rocking motion has been investigated by Pompei *et al.* (1998). In this study, it is assumed that the coefficient of friction between the block and its base is sufficiently large to prevent sliding at any instant in the rocking motion. Under a positive horizontal ground acceleration $\ddot{u}_g$, the block will initially rotate with a negative rotation, $\theta < 0$, and if it does not overturn, it will

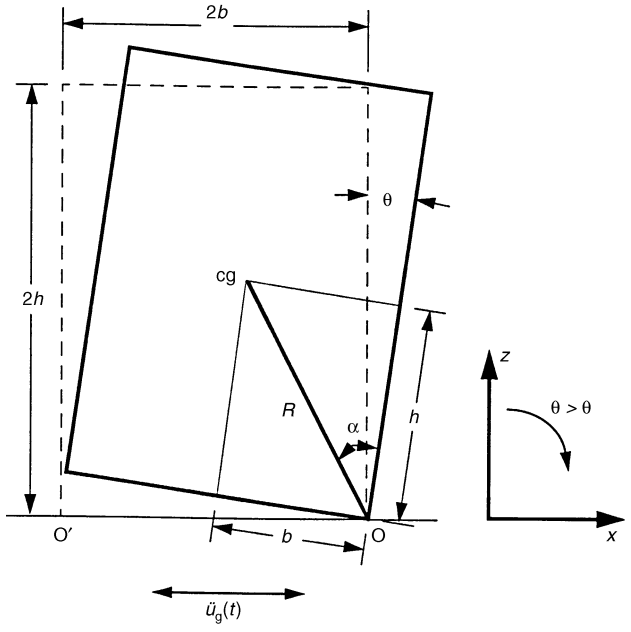

Fig. 1. Schematic of rocking block

eventually assume a positive rotation and so forth. Assuming zero vertical base acceleration ($\ddot{v}_g(t) = 0$), the equations of motion of a free-standing block with mass m are

$$I_O\ddot{\theta} + mgR\sin(-\alpha - \theta) = -m\ddot{u}_g R\cos(-\alpha - \theta),\ \theta < 0 \tag{1}$$

and

$$I_O\ddot{\theta} + mgR\sin(\alpha - \theta) = -m\ddot{u}_g R\cos(\alpha - \theta),\ \theta > 0 \tag{2}$$

For rectangular blocks, $I_O = (4/3)mR^2$, equations (1) and (2) can be expressed in the compact form

$$\ddot{\theta}(t) = -p^2\left\{\sin(\alpha\,\mathrm{sgn}[\theta(t)] - \theta(t)) + \frac{\ddot{u}_g}{g}\cos(\alpha\,\mathrm{sgn}[\theta(t)] - \theta(t))\right\} \tag{3}$$

where $p = \sqrt{(3g/4R)}$ is a quantity with units in rad/s, and sgn[ ] is the signum function. The larger the block is (larger R) the smaller p is. The oscillation frequency of a rigid block under free vibration is not constant, since it depends strongly on the vibration amplitude (Housner, 1963). Nevertheless, the quantity p is a measure of the dynamic characteristics of the block. For an electrical transformer, $p \approx 2$ rad/s, and for a household brick $p \approx 8$ rad/s.

When the block is rocking, it is assumed that the rotation continues smoothly from point O to O′. Conservation of momentum about point O′ just before the impact and right after the impact gives

$$I_O\dot{\theta}_1 - m\dot{\theta}_1 2bR\sin(\alpha) = I_O\dot{\theta}_2 \tag{4}$$

where $\dot{\theta}_1$ is the angular velocity just prior to the impact and $\dot{\theta}_2$ the angular velocity right after the impact. The ratio of kinetic energy after and before the impact is

$$r = \frac{\dot{\theta}_2^2}{\dot{\theta}_1^2} \tag{5}$$

which means that the angular velocity after the impact is only $\sqrt{r}$ times the velocity before the impact. Substitution of equation (5) into equation (4) gives

$$r = \left[1 - \frac{3}{2}\sin^2\alpha\right]^2 \tag{6}$$

The value of the coefficient of restitution given by equation (6) is the maximum value of r under which a block with slenderness α will undergo rocking motion. If additional energy is lost due to interface mechanisms, the value of the true coefficient of restitution, r, will be less than the one computed from equation (6). In this study, the entire analysis is conducted using the maximum value of the coefficient of restitution given by equation (6).

Equations (1) and (2) are well known in the literature (e.g. Yim *et al.*, 1980; Spanos & Koh, 1984; Hogan, 1989). They are valid for arbitrary values of the block angle α. For tall, slender blocks, the angle $\alpha = \tan^{-1}(b/h)$, is relatively small, and equations (1) and (2) can be linearized. Closed-form solutions of the linearized equations for harmonic excitation have been presented by Housner (1963) for positive rotations only ($\theta > 0$), and by Hogan (1989) for positive and negative rotations. Herein, the solution of the linearized equations is derived for a sinusoidal ground motion for both positive and negative rotations, in order to revisit the overturning conditions due to half-sine pulse that were postulated by Housner (1963) and to examine the rocking behaviour of rigid blocks subjected to cycloidal pulses. Within the limits of the linear approximation and for a harmonic ground acceleration with amplitude a_p and circular frequency ω_p:

$$\ddot{u}_g(t) = a_p\sin(\omega_p t + \psi) \tag{7}$$

Equations (1) and (2) become

$$\ddot{\theta}(t) - p^2\theta(t) = -\frac{a_p}{g}p^2\sin(\omega_p t + \psi) + p^2\alpha,\ \theta < 0 \tag{8}$$

and

$$\ddot{\theta}(t) - p^2\theta(t) = -\frac{a_p}{g}p^2\sin(\omega_p t + \psi) - p^2\alpha,\ \theta > 0 \tag{9}$$

where $\psi = \sin^{-1}(\alpha g/a_p)$ is the phase when rocking initiates. The integration of equations (8) and (9) gives

$$\theta(t) = A_1\sinh(pt) + A_2\cosh(pt) - \alpha + \frac{1}{1 + (\omega_p^2/p^2)}\frac{a_p}{g}\sin(\omega_p t + \psi),\ \theta < 0 \tag{10}$$

and

$$\theta(t) = A_3\sinh(pt) + A_4\cosh(pt) + \alpha + \frac{1}{1 + (\omega_p^2/p^2)}\frac{a_p}{g}\sin(\omega_p t + \psi),\ \theta > 0 \tag{11}$$

where

$$A_1 = A_3 = \frac{\dot{\theta}_O}{p} - \frac{\omega_p/p}{1 + \omega_p^2/p^2}\frac{a_p}{g}\cos(\psi) = \frac{\dot{\theta}_O}{p} - \alpha\frac{\omega_p/p}{1 + \omega_p^2/p^2}\frac{\cos(\psi)}{\sin(\psi)} \tag{12}$$

$$A_2 = \theta_O + \alpha - \frac{1}{1 + \omega_p^2/p^2}\frac{a_p}{g}\sin(\psi) = \theta_O + \alpha - \frac{\alpha}{1 + \omega_p^2/p^2} \tag{13}$$

$$A_4 = \theta_O - \alpha - \frac{1}{1 + \omega_p^2/p^2}\frac{a_p}{g}\sin(\psi) = \theta_O - \alpha - \frac{\alpha}{1 + \omega_p^2/p^2} \tag{14}$$

The time histories for the angular velocities are directly obtained from the time derivatives of equations (10) and (11):

$$\dot{\theta}(t) = pA_1\cosh(pt) + pA_2\sinh(pt) + \frac{\omega_p}{1 + (\omega_p^2/p^2)}\frac{a_p}{g}\cos(\omega_p t + \psi),\ \theta < 0 \tag{15}$$

and

$$\dot{\theta}(t) = pA_3\cosh(pt) + pA_4\sinh(pt) + \frac{\omega_p}{1 + (\omega_p^2/p^2)}\frac{a_p}{g}\cos(\omega_p t + \psi),\ \theta > 0 \tag{16}$$

The solution presented by Housner (1963) is a special case of the solution given by equation (10) to equation (14). Assuming zero initial rotation and zero initial angular velocity ($\theta(0) = \dot{\theta}(0) = 0$), the substitution of equations (12) and (13) into equation (10) gives

$$-\theta(t) = \alpha + \frac{\alpha}{1 + (\omega_p^2/p^2)}\left[\frac{\omega_p}{p}\frac{a_p}{\alpha g}\cos\psi\sin\psi - \frac{\omega_p^2}{p^2}\cosh(pt) - \frac{a_p}{\alpha g}\sin(\omega_p t + \psi)\right] \tag{17}$$

Recalling that $\sin\psi = \alpha g/a_p$, equation (17) takes the form

$$-\theta(t) = \alpha + \frac{\alpha}{1 + (\omega_p^2/p^2)} \times \left[\frac{\omega_p}{p}\frac{\cos\psi}{\sin\psi}\sinh(pt) - \frac{\omega_p^2}{p^2}\cosh(pt) - \frac{\sin(\omega_p t + \psi)}{\sin\psi}\right] \quad (18)$$

which is the solution reported by Housner (equation (10) in his paper). The minus sign on the left-hand side of equation (18) is there because we considered that the ground moves with a positive sine acceleration, and therefore that the block initially rotates with a negative angle $\theta(t) < 0$.

RESPONSE TO A HALF-SINE PULSE

The analytical solutions given by equations (10), (11), (15) and (16) can be used to compute the linear rocking response and the minimum acceleration amplitude of any sinusoidal excitation with finite duration that is needed to overturn a block. A solution for the minimum acceleration amplitude of a half-sine pulse that is needed to overturn a block was presented by Housner (1963). Unfortunately, the solution presented in that pioneering work and subsequently presented in later papers (Yim *et al.* (1980), among others) is incorrect. In this section, this flaw is rectified by establishing the correct conditions for a block to overturn.

In his seminal paper, Housner (1963) postulated that the condition for overturning is that the angle of rotation, θ, is equal to the angle α of the block at time $t = (\pi - \psi)/\omega_p$, which is the time at which the half-sine pulse expires. Based on this forced postulate, he derived a simple expression that provides the minimum acceleration amplitude required to overturn the block.

In reality, under the minimum overturning acceleration amplitude, the block will topple during its free vibration regime. This can be found by examining the free vibration response where the homogeneous part of the solution is expressed by equations (10) and (11) with $a_p = 0$. In the homogeneous solution, the initial rotation θ_O and initial angular velocity $\dot{\theta}_O$ in the integration constants, A_1 and A_2, are the rotation and angular velocity of the block at the instant when the sinusoidal excitation expires. Fig. 2 shows the response of a rigid block with dimensions $b = 0{\cdot}2$ m and $h = 0{\cdot}6$ m subjected to a half-sine pulse excitation with duration 0·5 s and excitation frequency $\omega_p = 2\pi$. On the left of Fig. 2, the amplitude of the acceleration pulse is $a_g = 5{\cdot}430\ \mathrm{m/s^2}$ ($0{\cdot}5535g$) and the block does not overturn, whereas on the right of Fig. 2, $a_g = 5{\cdot}440\ \mathrm{m/s^2}$ ($0{\cdot}5545g$) and the block overturns. The solid line is the analytical solution presented in the previous section, and the dashed line is the result of the numerical solution of the linearized equations of motion presented later in the paper. Fig. 2 illustrates that the overturning of the block happens much later than the time Housner (1963) had considered (end of the excitation pulse). Under the ideal condition that the block is being subjected to the exact value of the minimum acceleration needed to overturn it, the time when overturning occurs is infinitely large. Accordingly, the limit state condition for overturning is that the time when overturning occurs is arbitrarily large.

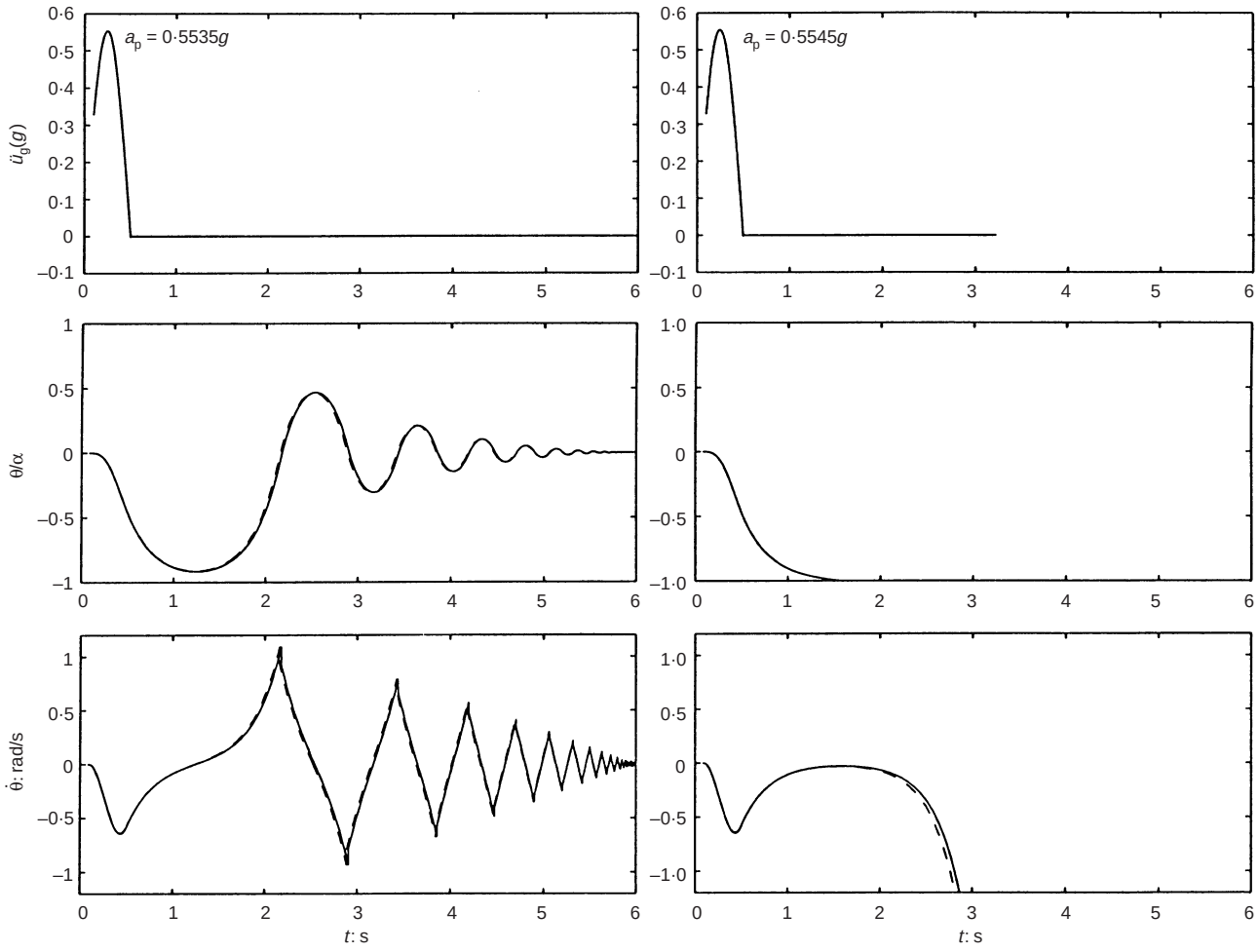

Fig. 2. Rotation and angular velocity time histories of a rigid block ($b = 0{\cdot}2$ m, $h = 0{\cdot}6$ m) subjected to a half-sine pulse excitation. Left: no overturning. Right: overturning. Solid line: analytical solution. Dashed line: numerical solution with linear formulation

The overturning condition of the block can be established by examining Fig. 2, which suggests that the block experiences the maximum rotation during the free vibration regime. Since the angle of rotation at the end of the excitation pulse is negative, the equation of motion during the free vibration regime that immediately follows is

$$\theta(t) = A_1 \sinh(pt) + A_2 \cosh(pt) - \alpha \tag{19}$$

where A_1 and A_2 are integration constants that depend on the rotation and angular velocity of the block at the end of the excitation pulse and are given by

$$A_1 = \frac{\dot{\theta}_O}{p},\ A_2 = \theta_O + \alpha \tag{20}$$

During this free vibration regime that immediately follows the forced vibration regime, the block will not overturn as long as the angular velocity decreases in magnitude monotonically, reaches zero and then increases, while the block rotates back to the equilibrium position. However, if the velocity does not reach zero, but instead reaches an extremum, the block will overturn. Accordingly, the block overturns when

$$\ddot{\theta}(t) = A_1 p^2 \sinh(pt) + A_2 p^2 \cosh(pt) = 0 \tag{21}$$

which gives

$$\tanh(pt) = -\frac{A_2}{A_1} \tag{22}$$

Our previous analysis revealed that under the critical acceleration, the time when overturning occurs is large enough for $\tanh(pt) = 1$, and the condition for overturning reduces to

$$A_1 + A_2 = 0 \tag{23}$$

The computation of A_1 and A_2 (see equations (12) and (13)) involves the evaluation of θ_O and $\dot{\theta}_O$ at the beginning of the free vibration regime, which occurs at time $t = (\pi - \psi)/\omega_p$. Consequently, θ_O and $\dot{\theta}_O$ are computed from equation (18) and its derivatives at time $t = (\pi - \psi)/\omega_p$. This gives

$$\theta_O = -\alpha - \frac{\alpha}{1 + (\omega_p^2/p^2)} \frac{\omega_p}{p} \times \left\{ \frac{\cos\psi}{\sin\psi} \sinh\left[\frac{p}{\omega_p}(\pi - \psi)\right] - \frac{\omega_p}{p} \cosh\left[\frac{p}{\omega_p}(\pi - \psi)\right] \right\} \tag{24}$$

$$\dot{\theta}_O = \frac{-\alpha p}{1 + (\omega_p^2/p^2)} \frac{\omega_p}{p} \times \left\{ \frac{\cos\psi}{\sin\psi} \cosh\left[\frac{p}{\omega_p}(\pi - \psi)\right] - \frac{\omega_p}{p} \sinh\left[\frac{p}{\omega_p}(\pi - \psi)\right] + \frac{1}{\sin\psi} \right\} \tag{25}$$

With the substitution of equations (24) and (25) into equations (12) and (13), (23) takes the form

$$\cos\psi \cosh\left[\frac{p}{\omega_p}(\pi - \psi)\right] - \frac{\omega_p}{p} \sin\psi \sinh\left[\frac{p}{\omega_p}(\pi - \psi)\right] + 1 + \cos\psi \sinh\left[\frac{p}{\omega_p}(\pi - \psi)\right] - \frac{\omega_p}{p} \sin\psi \cosh\left[\frac{p}{\omega_p}(\pi - \psi)\right] = 0 \tag{26}$$

Equation (26) can be further simplified by using the definition of the hyperbolic functions: $\cosh x = (e^x + e^{-x})/2$ and $\sinh x = (e^x - e^{-x})/2$. This gives

$$\frac{\omega_p}{p} \sin\psi - \cos\psi = \exp(-p/\omega_p(\pi - \psi)) \tag{27}$$

Equation (27) is the condition for overturning. The solution of this transcendental equation gives the value of ψ for which the acceleration $a_{pO} = \alpha g/\sin\psi$ is the minimum acceleration needed to overturn the block. Fig. 3(a) shows with a solid line

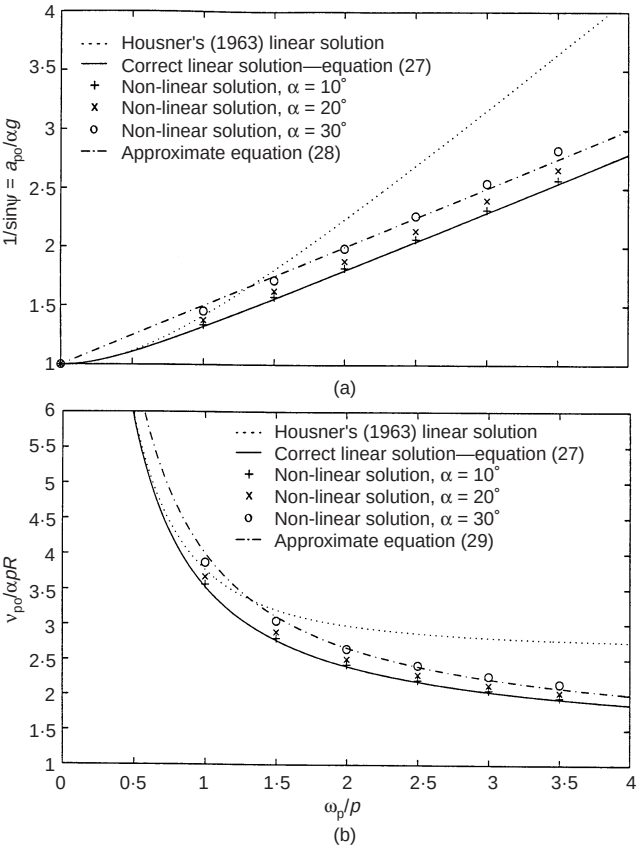

Fig. 3. (a) Spectrum of the minimum acceleration amplitude, a_{po}, of a half-sine pulse needed to overturn a free-standing block. (b) Spectrum of the minimum velocity amplitude, v_{po}, of a half-sine pulse needed to overturn a free-standing block

the solution of equation (27) as a function of ω_p/p and is compared with the unconservative solution presented by Housner (1963) (dotted line). Equation (27) was derived independently by Shi *et al.* (1996), who stated correctly that under the minimum acceleration needed to overturn the block, the kinetic energy of the block at the verge of overturning should be zero.

The points shown in Fig. 3 are the numerical solutions for different values of the block slenderness obtained with a non-linear formulation that is presented later in the paper. Fig. 3(a) also illustrates that, in the low-frequency range, the minimum overturning acceleration amplitude is a nearly linear function of ω_p/p (chain line). A dependable approximation of the correct solution is

$$\frac{a_{po}}{\alpha g} \approx 1 + \frac{1}{2}\frac{\omega_p}{p} \tag{28}$$

At the end of the half-sine pulse, the ground has reached the constant velocity $v_p = 2a_p/\omega_p$. For a rectangular block, $p = \sqrt{[3g/(4R)]}$, equation (28) offers a dependable approximation for the minimum overturning velocity amplitudes:

$$v_{po} = \frac{a_p T_p}{\pi} \approx 2\alpha \left(\frac{T_p g}{2\pi} + \sqrt{\frac{Rg}{3}} \right) \tag{29}$$

The results of the approximate expression given by equation (29) are shown in Fig. 3(b) next to the exact linear solution (solid line), the numerical solution (points) and the unconservative solution presented by Housner (1963).

Equation (29) shows that in the low frequency range $\omega_p/p < 3$, the minimum overturning velocity amplitude depends not only on the slenderness α and the size R, but also on the duration of the pulse. Consequently, if one considers two different half-sine acceleration pulses with the same product $a_p T_p$,

the short-period pulse with the larger acceleration amplitude is more capable of overturning a block than the longer-period pulse with the smaller acceleration amplitude.

CLOSED-FORM APPROXIMATION OF NEAR-SOURCE GROUND MOTIONS

During the last two decades, an ever-increasing database of recorded earthquakes has demonstrated that the dynamic characteristics of the ground near the faults of major earthquakes have distinguishable long-duration pulses. Near-source ground motions contain large displacement pulses, say one or two coherent pulses from 0·5 m to more than 1·5 m. Their duration is usually between 1 and 3 s but it can be as long as 6 s. What makes these motions particularly destructive to a variety of structures is not only their occasionally high peak ground acceleration but also the area under the relatively long-duration acceleration pulse. This area represents the 'incremental' ground velocity which is the net increment of the ground velocity along a monotonic segment of its time history. Such velocity increments are of the order of 0·5m/s or even higher. Although they do not happen fast enough to generate excessive ground accelerations, they happen just at the right pace to generate devastating shear forces at the base of flexible structures (Anderson & Bertero, 1986). Of particular interest are the forward motions, the forward-and-back motions, motions that exhibit one main cycle in their displacement histories, and motions that exhibit two main cycles in their displacement histories.

Figure 4 (left) shows the fault parallel components of the acceleration, velocity and displacement histories of the 18 June 1992 Landers earthquake recorded at the Lucerne Valley station (Iwan & Chen, 1994). The motion resulted in a forward displacement of the order of 1·8 m. The coherent long-duration pulse responsible for most of this displacement can also be distinguished in the velocity history, whereas, the acceleration history is crowded with high-frequency spikes. Fig. 4 (right) plots the acceleration, velocity and displacement histories of a type A cycloidal pulse given by (Jacobsen & Ayre, 1958; Makris, 1997)

$$\ddot{u}_g(\tau) = \omega_p \frac{v_p}{2} \sin(\omega_p \tau),\ 0 \leqslant \tau \leqslant T_p \tag{30}$$

$$\dot{u}_g(\tau) = \frac{v_p}{2} - \frac{v_p}{2} \cos(\omega_p \tau),\ 0 \leqslant \tau \leqslant T_p \tag{31}$$

$$u_g(\tau) = \frac{v_p}{2}\tau - \frac{v_p}{2\omega_p} \sin(\omega_p \tau),\ 0 \leqslant \tau \leqslant T_p \tag{32}$$

where $\tau = t - t_0$ with t_0 being the time in the record when the trigonometric pulse initiates. In constructing Fig. 4 (right), the values of $T_p = 7{\cdot}0$ s and $v_p = 0{\cdot}5$ m/s were used; these are approximations of the duration and velocity of the main pulse. Fig. 4 indicates that a simple one-sine pulse can capture some of the kinematic characteristics of the motion recorded at the Lucerne Valley station. On the other hand, the resulting acceleration amplitude, $a_p = \omega_p v_p/2 \approx 0{\cdot}045g$, is one order of magnitude smaller than the recorded peak ground acceleration.

Figure 5 (left) shows the acceleration, velocity and displacement histories of the fault normal motions recorded at the El Centro Station, array no. 5, during the 15 October 1979 Imperial Valley earthquake. This motion resulted in a forward-and-back pulse with a 3·2 s duration. In this case, the coherent long-period pulse is distinguishable not only in the displacement and velocity record, but also in the acceleration record. Fig. 5 (right) shows the acceleration, velocity and displacement histories of a type B cycloidal pulse given by Makris (1997):

$$\ddot{u}_g(\tau) = \omega_p v_p \cos(\omega_p \tau),\ 0 \leqslant \tau \leqslant T_p \tag{33}$$

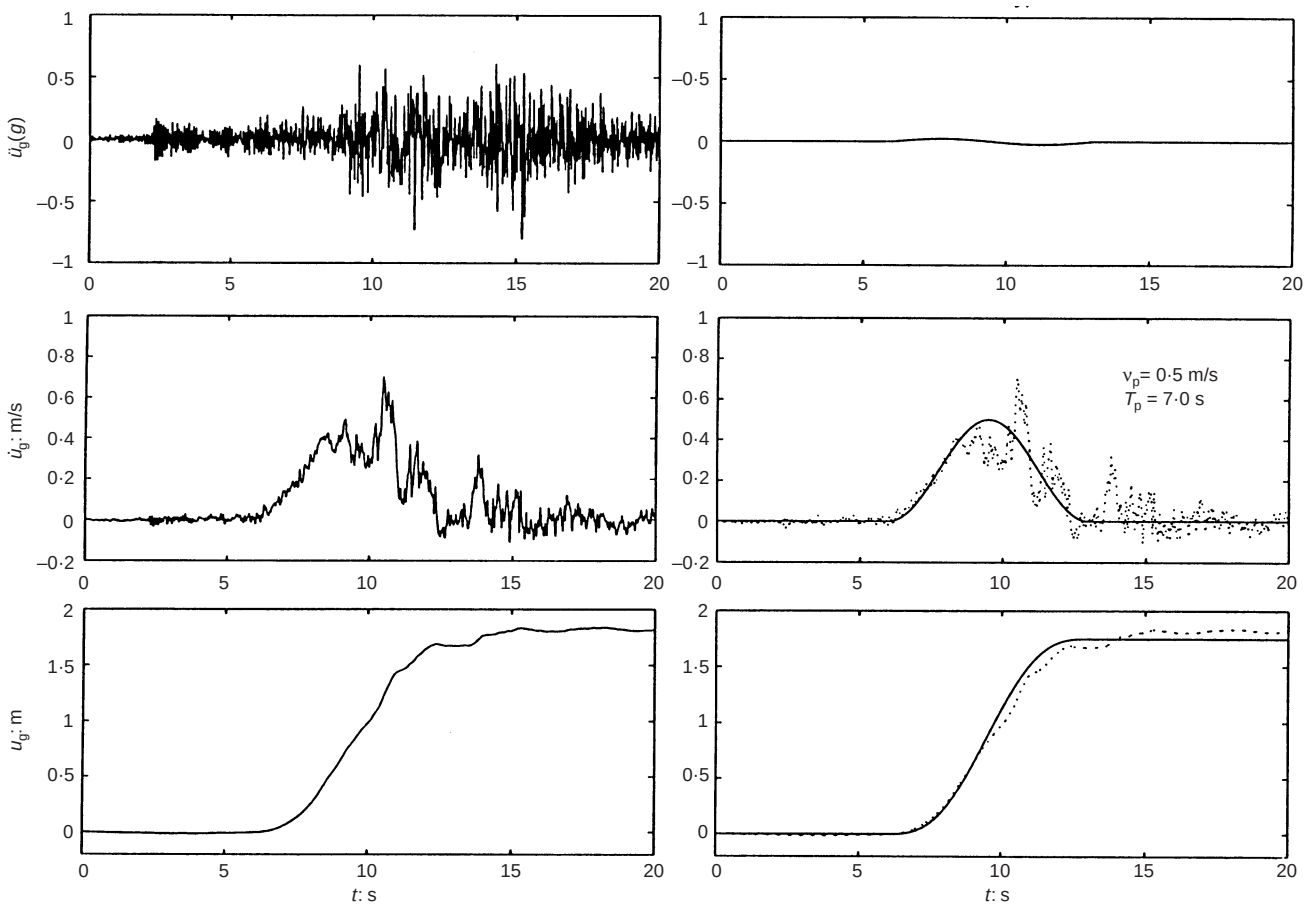

Fig. 4. Fault parallel components of the acceleration, velocity and displacement time histories recorded at the Lucerne Valley station during the 28 June 1992 Landers, California earthquake (left), and a cycloidal type A pulse (right)

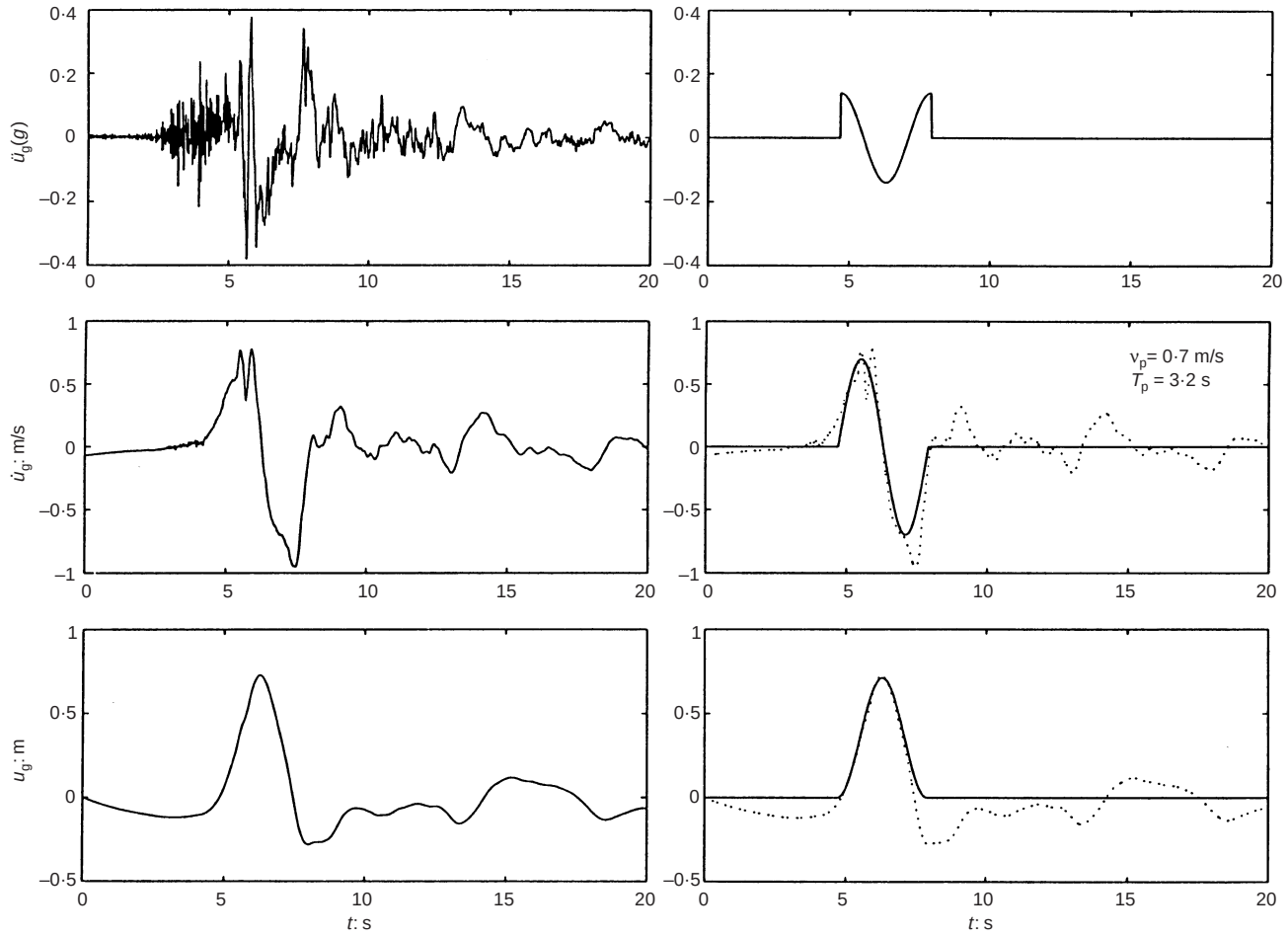

Fig. 5. Fault normal components of the acceleration, velocity and displacement time histories recorded at the El Centro Array no. 5 station during the 15 October 1979 Imperial Valley, California earthquake (left), and a cycloidal type B pulse (right)

$$\dot{u}_g(\tau) = v_p \sin(\omega_p \tau),\ 0 \leqslant \tau \leqslant T_p \tag{34}$$

$$u_g(\tau) = \frac{v_p}{\omega_p} - \frac{v_p}{\omega_p}\cos(\omega_p \tau),\ 0 \leqslant \tau \leqslant T_p \tag{35}$$

where again $\tau = t - t_0$, and t_0 is the time in the record when the trigonometric pulse initiates. In constructing Fig. 5 (right), the values of $T_p = 3{\cdot}2$ s and $v_p = 0{\cdot}7$ m/s were used as approximate values of the pulse period and velocity amplitude of the recorded motions shown in Fig. 5 (left).

Figure 6 (left) portrays the fault normal components of the acceleration, velocity and displacement histories recorded the 17 January 1994 Northridge earthquake recorded at the Rinaldi station. This motion resulted in a forward ground displacement that recovered partially. Accordingly, the fault normal component of the Rinaldi station record is in between a forward and a forward-and-back pulse. Fig. 6 (centre) shows the results of equations (30) to (32) by assuming a pulse duration $T_p = 0{\cdot}8$ s and a velocity amplitude $v_p = 1{\cdot}75$ m/s, which are approximations of the duration and velocity amplitude of the first main pulse shown on the record. Fig. 6 (right) shows the results of equations (33) to (35) by considering a pulse duration $T_p = 1{\cdot}3$ s and a velocity amplitude $v_p = 1{\cdot}3$ m/s.

Not all records are forward or forward-and-back pulses. Fig. 7 (left) portrays the fault normal component of the acceleration, velocity and displacement time histories recorded at the Sylmar station during 17 January 1994 Northridge earthquake. The ground displacement consists of two main long-period cycles, the first cycle being the largest, and the subsequent ones decaying. These long-period pulses are also distinguishable in the ground velocity history, where the amplitude of the positive pulses is larger than the amplitude of the negative pulses. Near-fault ground motions, where the displacement history exhibits one or more long-duration cycles, are approximated with type C pulses. An n-cycle ground displacement is approximated with a type C_n pulse that is defined as

$$\ddot{u}_g(\tau) = \omega_p v_p \sin(\omega_p \tau + \varphi),$$
$$0 \leqslant \tau \leqslant \left(n + \frac{1}{2} - \frac{\varphi}{\pi}\right) T_p \tag{36}$$

$$\dot{u}_g(\tau) = v_p \cos(\omega_p \tau + \varphi) - v_p \sin(\varphi),$$
$$0 \leqslant \tau \leqslant \left(n + \frac{1}{2} - \frac{\varphi}{\pi}\right) T_p \tag{37}$$

$$u_g(\tau) = -\frac{v_p}{\omega_p}\cos(\omega_p \tau + \varphi) - v_p \tau \sin(\varphi) + \frac{v_p}{\omega_p}\cos(\varphi),$$
$$0 \leqslant \tau \leqslant \left(n + \frac{1}{2} - \frac{\varphi}{\pi}\right) T_p \tag{38}$$

In deriving these expressions, it was required that the displacement and velocity be differentiable signals. The value of the phase angle, φ, is determined by requiring that the ground displacement at the end of the pulse is zero. A type C_n pulse with frequency $\omega_p = 2\pi/T_p$ has a duration $T = (n + 1/2)T_p - 2\varphi/\omega_p = (n + 1/2 - \varphi/\pi)T_p$. In order to have a zero ground displacement at the end of a type C_n pulse

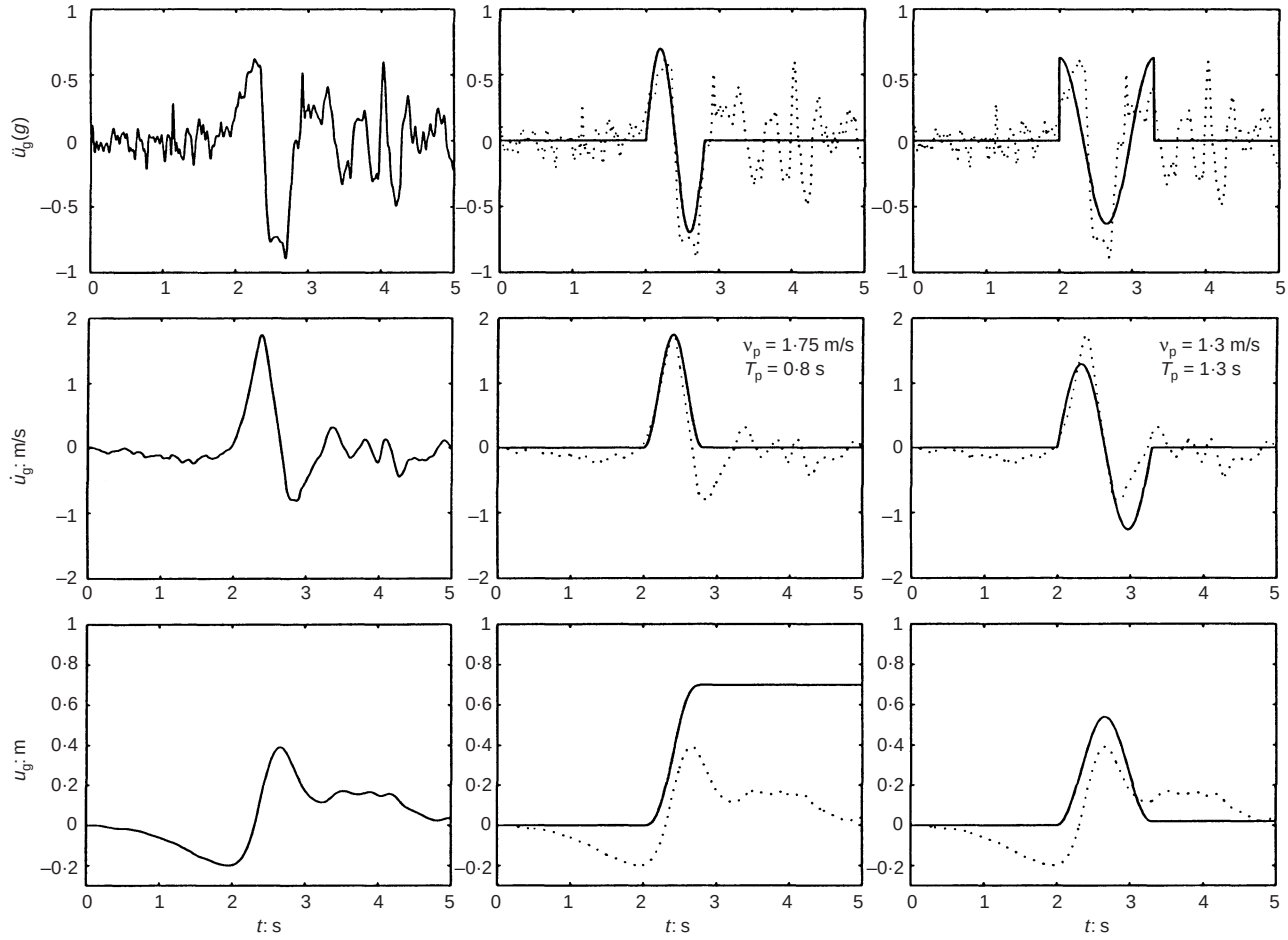

Fig. 6. Fault normal components of the acceleration, velocity and displacement time histories recorded at the Rinaldi station during the 17 January 1994 Northridge, California earthquake (left), a cycloidal type A pulse (centre) and a cycloidal type B pulse (right)

$$\int_0^{(n+1/2-\varphi/\pi)T_p} \ddot{u}_g(t)\,\mathrm{d}t = 0 \tag{39}$$

Equation (39), after evaluation of the integral, gives

$$\cos[(2n+1)\pi-\varphi] + [(2n+1)\pi - 2\varphi]\sin\varphi - \cos\varphi = 0 \tag{40}$$

The solution of the transcendental equation given by equation (40) gives the value of the phase φ. As an example, for a type C_1 pulse ($n=1$) $\varphi = 0{\cdot}0697\pi$, whereas for a type C_2 pulse ($n=2$), $\varphi = 0{\cdot}0410\pi$. Fig. 8 (third and fourth column) shows the acceleration, velocity and displacement histories of a type C_1 and type C_2 pulse.

As n increases, a type C_n pulse tends to a harmonic steady-state excitation. Fig. 8 summarizes the acceleration, velocity and displacement shapes of a forward pulse, a forward-and-back pulse, a type C_1 pulse and a type C_2 pulse. The displacement of a forward-and-back pulse has the same shape as the velocity of a forward pulse. Similarly, the displacement of a type C_1 pulse resembles the shape of the velocity of a forward-and-back pulse and the shape of the acceleration of a forward pulse. This shows that type C pulses provide a continuous transition from cycloidal pulses to harmonic steady-state motions.

RESPONSE TO TRIGONOMETRIC PULSES

The previous section indicates that the kinematic characteristics of certain near-source ground motions can be approximated with simple trigonometric pulses. In this section, the overturning potential of type A, type B, type C_1 and type C_2 pulses is examined, and simple approximate expressions are derived which can provide valuable information on the overturning potential of recorded ground motions.

Response to a one-sine pulse (type A pulse)

Forward (non-reversing) ground displacements can be described with a one-sine pulse also known as a cycloidal pulse of type A, derived from equations (30) to (32). The linear rocking response of a rigid block subjected to a one-sine pulse can be computed with equations (10), (11), (15) and (16). Fig. 9 shows the response of a rigid block ($b = 0{\cdot}5$ m and $h = 1{\cdot}5$ m) subjected to a one-sine pulse excitation with duration of 1 s ($\omega_p = 2\pi$). The solid line is the result of the analytical solution and the dashed line is the result of the linear formulation of the numerical solution presented in the next section. The agreement between the two solutions validates the performance of the numerical algorithm. On the left of Fig. 9, the amplitude of the acceleration pulse is $a_p = 4{\cdot}426$ m/s^2 ($0{\cdot}4513g$) and the block does not overturn, whereas on the right of Fig. 9, $a_p = 4{\cdot}429$ m/s^2 ($0{\cdot}4514g$) and the block overturns. Fig. 9 indicates that under a one-sine input the block overturns at the end of the third quarter cycle after experiencing one impact. This reversal of the angle of rotation before overturning does not allow for the derivation of a closed-form expression that will yield the minimum acceleration needed to overturn the block. It becomes clear, however, that under a type A pulse the value of the coefficient of restitution affects the value of the critical overturning acceleration, since the block experiences

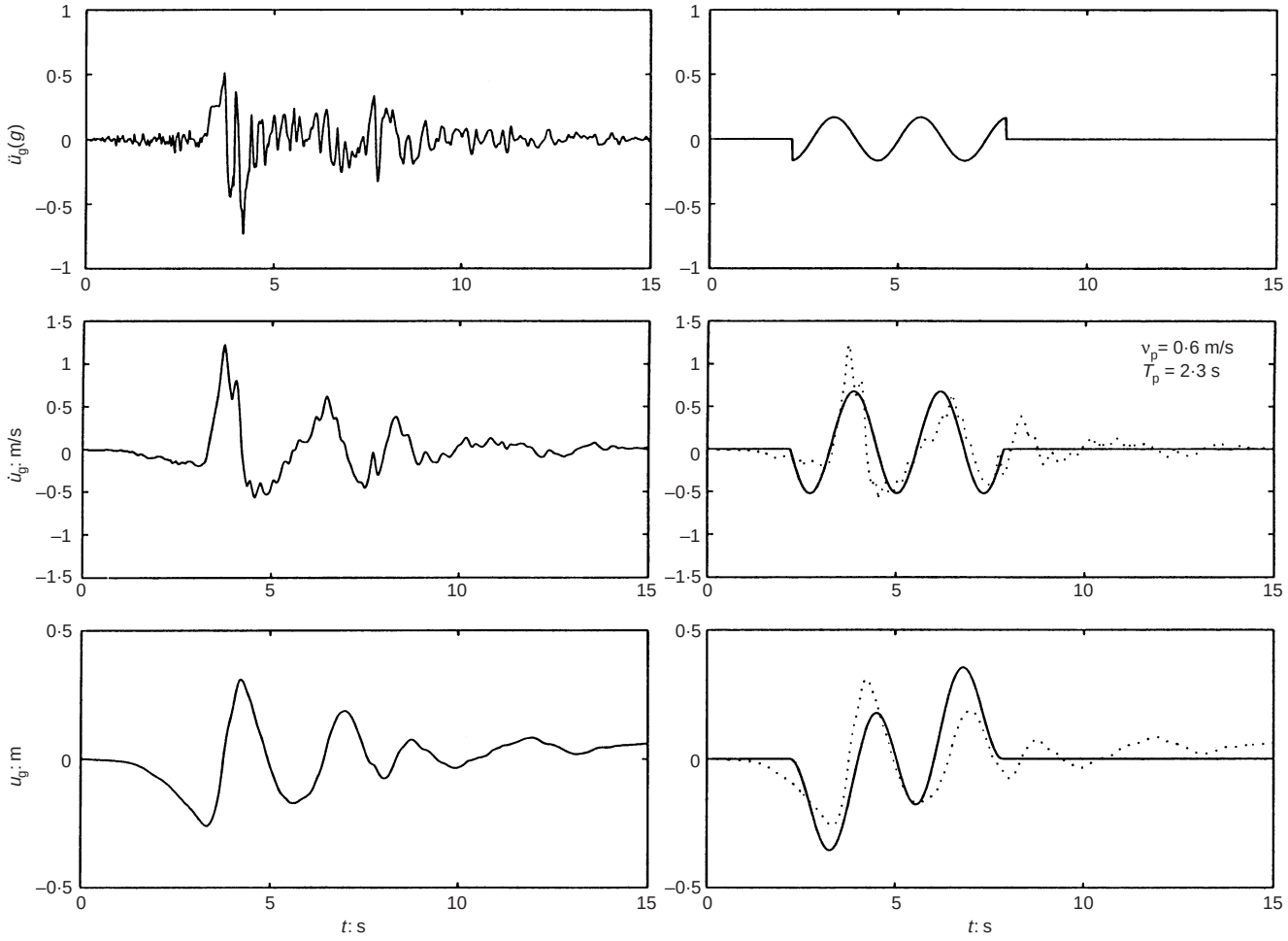

Fig. 7. Fault normal components of the acceleration, velocity and displacement time histories recorded at the Sylmar station during the 17 January 1994 Northridge, California earthquake (left), and a cycloidal type C_2 pulse (right)

one impact before overturning. Consequently, even the linear solution for the minimum overturning accelerations is angle dependent, since the coefficient of restitution, r, is a function of the slenderness of the block, α. The results presented herein are for the maximum value of the coefficient of restitution given by equation (6).

The minimum acceleration amplitude, a_{po}, of a one-sine pulse needed to overturn a rigid block with slenderness α, is plotted in Fig. 10(a). Results are computed for $\alpha = 10°$, 20° and 30° with the non-linear formulation that is presented in the last section and are compared with the linear solution for the minimum overturning acceleration of a half-sine excitation (equation (26)). It is shown that for a one-sine pulse (type A pulse), a considerably smaller acceleration amplitude is needed to overturn a block, since in this case the ground decelerates during the second half of the pulse. It is observed that the solution for $\alpha = 30°$ exhibits a stiffening effect for $\omega_p/p > 2{\cdot}5$, while for $\alpha \leqslant 20°$, Fig. 10 indicates that the minimum overturning acceleration amplitude, a_{po} is a nearly linear function of ω_p/p in the low-frequency range ($\omega_p/p < 3{\cdot}0$), which can be approximated with

$$\frac{a_{po}}{\alpha g} \approx 1 + \frac{1}{6}\frac{\omega_p}{p} \tag{41}$$

From equation (30), the velocity amplitude of the one-sine pulse is $v_p = 2a_p/\omega_p$, and for a slender rectangular block the minimum overturning velocity amplitude v_{po} of a one-sine pulse can be approximated with

$$v_{po} = \frac{a_{po}T_p}{\pi} \approx 2\alpha\left(\frac{T_p g}{2\pi} + \frac{1}{3}\sqrt{\frac{Rg}{3}}\right) \tag{42}$$

The results of the approximate expression given by equation (42) are shown in Fig. 10(b), next to the results derived from the non-linear numerical solution. The multiplication factor $1/3$ of the size term in equation (42) indicates that the size of the block, R, has a weaker effect in preventing toppling than in the case of a half-sine pulse.

Response to a one-cosine pulse (type B pulse)

While some near-source ground motions result in a forward pulse (non-reversing pulse), other near-source ground motions result in a forward-and-back pulse, where the ground dislocation recovers either fully or partially. In the previous section it was shown that many of the features of these forward-and-back pulses can be captured with a one-cosine pulse (type B pulse). Fig. 11 plots the response of the rigid block ($b = 0{\cdot}5$ m and $h = 1{\cdot}5$ m) subjected to a one-cosine pulse excitation with a duration of 1 s ($\omega_p = 2\pi$) and acceleration amplitudes slightly below and slightly above the critical overturning acceleration, a_{po}. The minimum acceleration amplitudes, a_{po}, of a one-cosine pulse needed to overturn a rigid block with slenderness α, are shown in Fig. 12(a). Results are computed for $\alpha = 10°$, 20° and 30° with the non-linear formulation that is presented in the next section.

Figure 12(a) also indicates that the minimum overturning acceleration amplitude of a one-cosine pulse needed to overturn

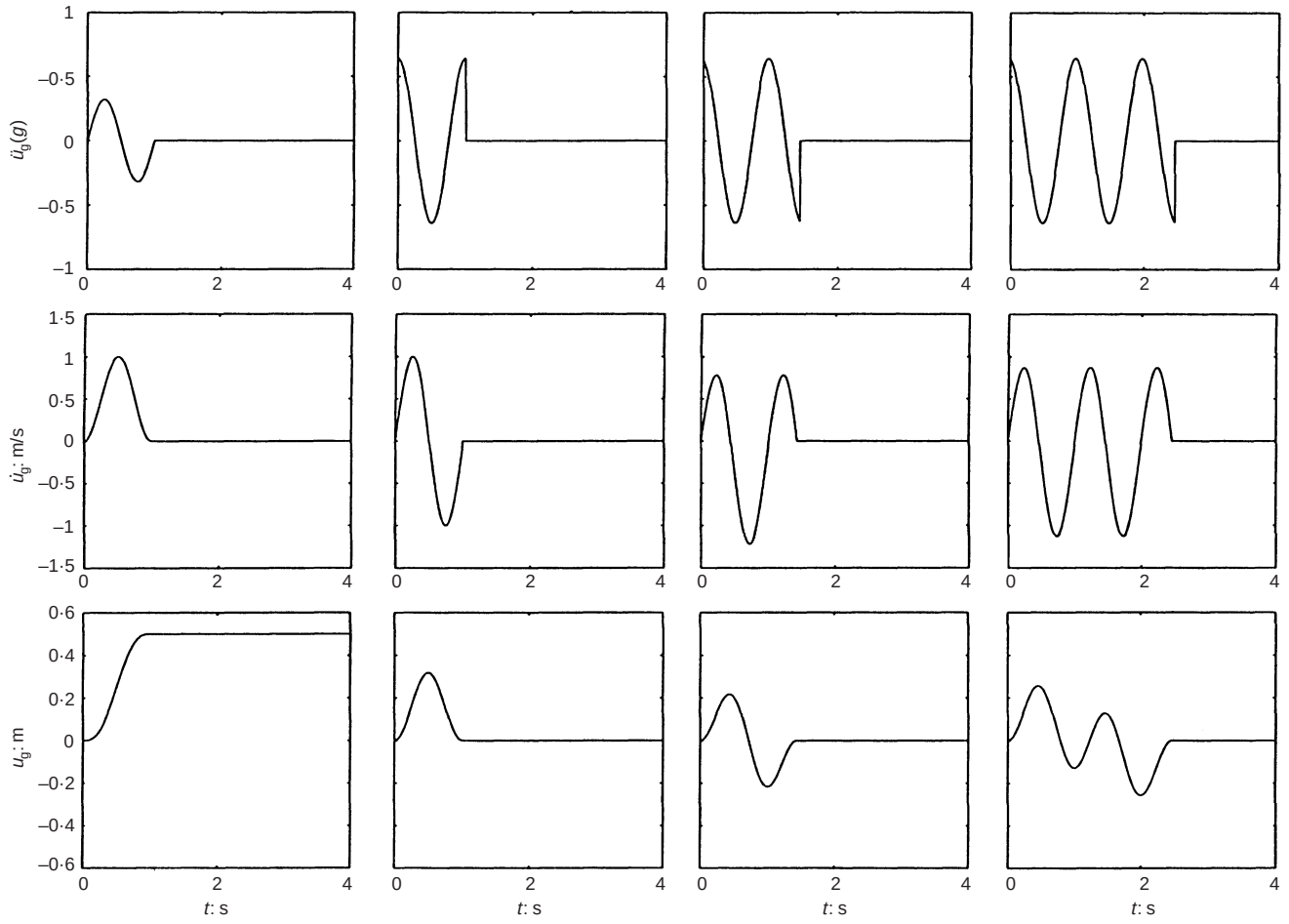

Fig. 8. Acceleration, velocity and displacement time histories of cycloidal pulses type A (first column), type B (second column), type C_1 (third column) and type C_2 (fourth column)

a block with an average slenderness of $\alpha = 20°$ can be approximated with the linear expression

$$\frac{a_{po}}{\alpha g} \approx 1 + \frac{1}{4}\frac{\omega_p}{p} \tag{43}$$

From equation (33), the velocity amplitude of the one-cosine pulse is $v_p = a_p/\omega_p$ and for a rectangular block equation (43) gives

$$v_{po} = \frac{a_{po} T_p}{\pi} \approx \alpha\left(\frac{T_p g}{2\pi} + \frac{1}{2}\sqrt{\frac{Rg}{3}}\right) \tag{44}$$

The results of the approximate expression given by equation (44) are shown in Fig. 12(b), next to the results derived from the non-linear numerical solution.

Response to type C pulses

The minimum acceleration amplitudes a_{po} of a type C_1 and a type C_2 pulse needed to overturn a block with slenderness $\alpha = 20°$ are shown in Fig. 13(a). For values of $\omega_p/p > 2{\cdot}0$, the acceleration values increase with frequency at a larger rate. However, for values of $\omega_p/p \leqslant 2{\cdot}0$, Fig. 13(a) indicates that the minimum overturning acceleration amplitudes for both type C_1 and type C_2 pulses are nearly linear functions of ω_p/p, which can be approximated with

$$\frac{a_{po}}{\alpha g} \approx 1 + \frac{1}{6}\frac{\omega_p}{p} \tag{45}$$

The relation given by equation (45) is the same as the relation given by equation (41), which was derived for a type A pulse. For type C pulses, equations (36) and (37) give the velocity amplitude as $v_p = a_p/\omega_p$ which is half the velocity amplitude that one obtains from a type A pulse with the same acceleration amplitude a_p. Accordingly, for a slender block, the minimum overturning velocity amplitude of either a type C_1 or type C_2 pulse can be approximated with

$$v_{po} = \frac{a_{po} T_p}{\pi} \approx \alpha\left(\frac{T_p g}{2\pi} + \frac{1}{3}\sqrt{\frac{Rg}{3}}\right) \tag{46}$$

The results of the approximate expressions given by equation (46) are shown in Fig. 13(b), next to results obtained with the non-linear numerical solution for $\alpha = 20°$.

RESPONSE TO SEISMIC EXCITATION

The rocking response of a rigid block subjected to earthquake excitation is computed numerically via a state-space formulation which can accommodate the non-linear nature of the problem. Similar integration of the equation of motion has been carried out by Yim *et al.* (1980), Spanos & Koh (1984), and Hogan (1989), among others. The state vector of the system is merely

$$\{y(t)\} = \begin{Bmatrix} \theta(t) \\ \dot{\theta}(t) \end{Bmatrix} \tag{47}$$

and the time-derivative vector, $\{f(t)\}$, is

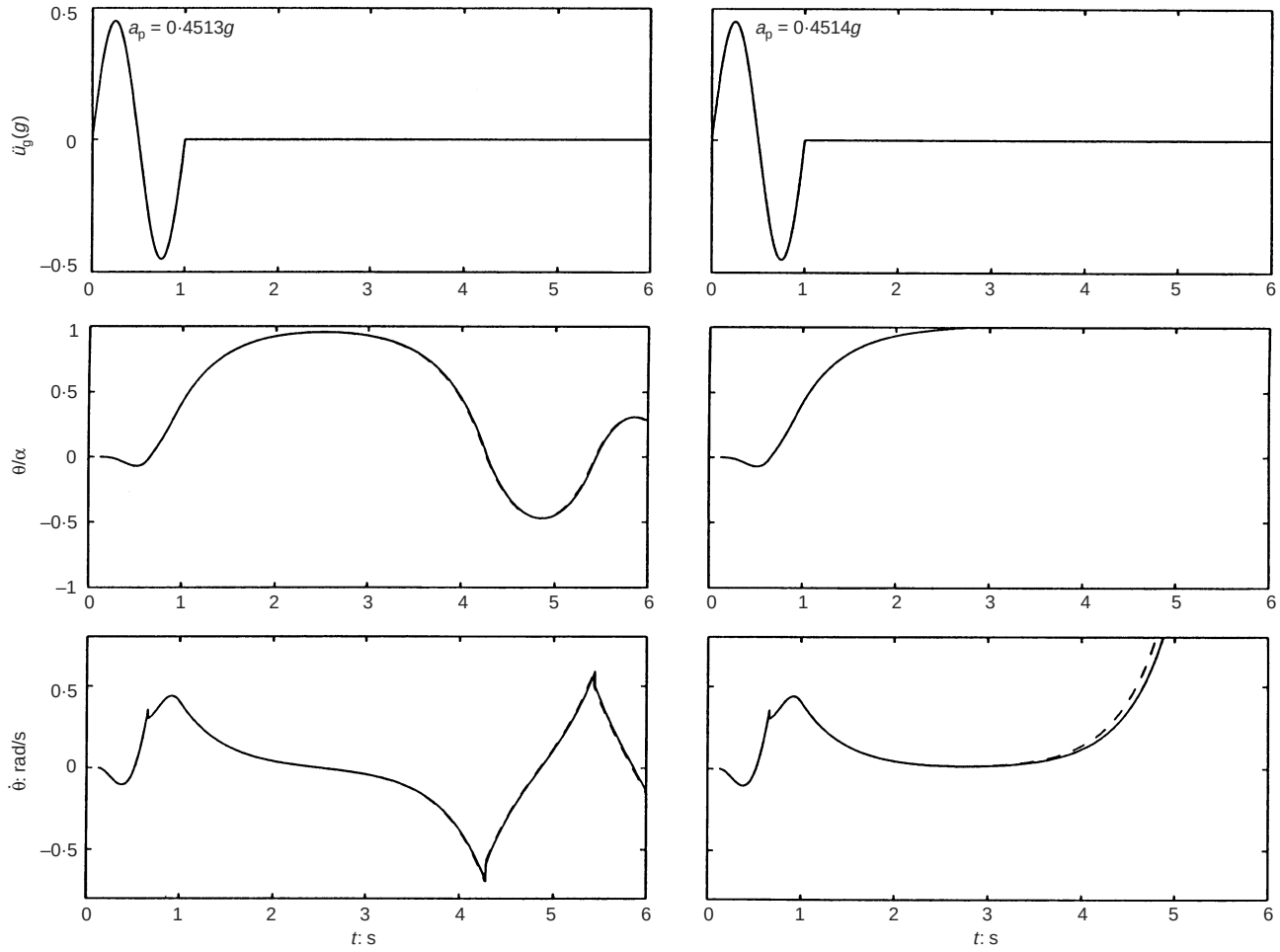

Fig. 9. Rotation and angular velocity time histories of a rigid block ($b = 0{\cdot}5$ m, $h = 1{\cdot}5$ m) subjected to a one-sine pulse excitation. Left: no overturning. Right: overturning. Solid lines: analytical solution. Dashed lines: numerical solution with linear formulation

$$\{f(t)\} = \{\dot{y}(t)\} = \begin{Bmatrix} \dot{\theta}(t) \\ -p^2\left[\sin(\alpha\,\mathrm{sgn}[\theta(t)] - \theta(t)) + \dfrac{\ddot{u}_g}{g}\cos(\alpha\,\mathrm{sgn}[\theta(t)] - \theta(t))\right] \end{Bmatrix} \tag{48}$$

For slender blocks, the linear approximation becomes dependable, and equation (48) reduces to

$$\{f(t)\} = \{\dot{y}(t)\} = \begin{Bmatrix} \dot{\theta}(t) \\ p^2\left[-\alpha\,\mathrm{sgn}[\theta(t)] + \theta(t) - \dfrac{\ddot{u}_g(t)}{g}\right] \end{Bmatrix} \tag{49}$$

The numerical integration of equation (48) or (49) is performed with standard ODE solvers available in MATLAB (1992). The fidelity of the numerical algorithm is validated in Fig. 9, where the numerical solution of the linear equations of motion given by equation (49) (dashed lines) is compared with the analytical solution given by equations (10) and (11), and equations (15) and (16) (solid lines). With the non-linear formulation given by equation (48), the effects of the non-linear nature of the problem are captured. As an example, the true minimum acceleration amplitudes of a half-sine pulse needed to overturn rigid blocks with various geometries are shown in Fig. 3 and are compared with the correct linear solution given by equation (26) and the unconservative linear solution given by Housner (1963).

In the foregoing section, we analysed the rocking response of a free-standing block subjected to three types of trigonometric pulses that can approximate some of the kinematic characteristics of near-source ground motions. We derived expressions to express the minimum overturning acceleration and velocity amplitudes of these pulses, and we concluded that for small values of the frequency ratio ($\omega_p/p < 3$), the toppling of a block depends on its slenderness, α, its size, R, and the duration of the pulse, T_p. In this section, the foregoing analysis is used to provide information on the stability of a block subjected to near-source ground motions.

The challenge with such motions is that on many occasions the main long-duration pulse that generates the large ground displacements is jammed by high-frequency fluctuations. For instance, this phenomenon is most apparent in the Lucerne Valley records, shown in Fig. 4. The El Centro Array no. 5 record, shown in Fig. 5, contains few distinct fluctuations on top of the main pulse, whereas the Rinaldi station record shown in Fig. 6, is clear enough to the extent that the pulse motion is distinguishable even in the acceleration history.

Figure 6 indicates that the Rinaldi station record is in between a 0·8 s type A pulse and a 1·3 s type B pulse. From equation (42), the minimum overturning velocity amplitude of a one-sine pulse with $T_p = 0{\cdot}8$ s that is needed to overturn the $0{\cdot}5\text{m} \times 1{\cdot}5$ m block ($\alpha = 18{\cdot}45° = 0{\cdot}3217$ rad, $p = 2{\cdot}157$ rad/s) is $v_p = 1{\cdot}29$ m/s. Accordingly, since the velocity amplitude of the Rinaldi station when considered as a forward pulse is approximately 1·75 m/s, the approximation of the Rinaldi station motion with a one-sine pulse shows that 74% ($1{\cdot}29/1{\cdot}75 = 0{\cdot}74$) of the Rinaldi motion is sufficient to overturn the block. On the other hand, equation (44) indicates that the minimum overturning velocity amplitude of a one-cosine pulse with $T_p = 1{\cdot}3$ s that is needed to overturn the

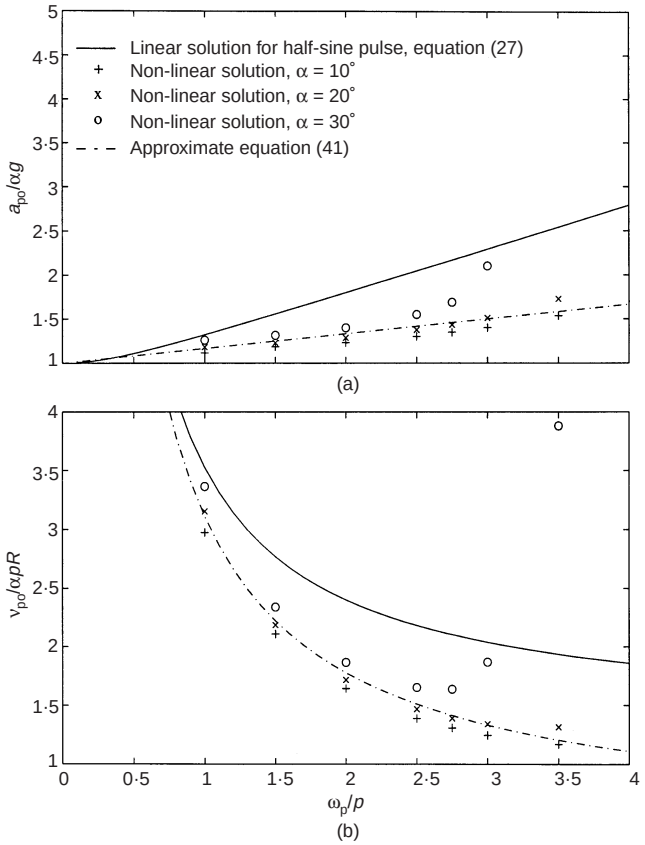

Fig. 10. Spectrum of the minimum acceleration amplitude (a) and velocity amplitude (b) of a one-sine type A pulse needed to overturn a free-standing block

same block is $v_p = 1{\cdot}02$ m/s. Now the approximation of the Rinaldi station to a one-cosine pulse shows that 78% ($1.02/1{\cdot}30 = 0{\cdot}78$) of the Rinaldi motion is sufficient to overturn the block. Fig. 14 (left) shows the rocking response of the $0{\cdot}5$ m $\times$ $1{\cdot}5$ m block subjected to the 75% level of the Rinaldi station motion, where the block does not overturn; whereas, on the right of Fig. 4, the block overturns when subjected to a 76% level of the Rinaldi station record. This level of 76% is between the levels of 74% and 78% that we computed with equations (42) and (43) respectively. Fig. 15 shows the minimum overturning velocity spectrum of the Rinaldi station motion by assuming a pulse frequency $\omega_p^A = 2\pi/0{\cdot}8$ s $= 2{\cdot}5\pi$ rad/s. The velocity spectrum of a pulse type A together with the solution of the approximate expression given by equation (42) are also shown in Fig. 5. The good agreement of the results presented in Fig. 5 indicates that the response values obtained from cycloidal pulses can provide dependable information on the overturning potential of recorded ground motions that contain a distinct, clean pulse.

Our analysis proceeds by investigating the rocking response of blocks to near-source ground motions that contain a distinct long-duration pulse as well as high-frequency fluctuations that override the long-duration pulse. The question that arises with such records is whether a block will overturn due to the high-frequency spike or due to the low acceleration, low-frequency pulse.

This question is partially addressed by observing the forward-and-back motion recorded at the El Centro, Array no. 5 station shown in Fig. 5. At approximately 5·5 s, the velocity history displays a distinct fluctuation which is distinguishable in the acceleration history. Fig. 16 zooms into the El Centro, Array no. 5 station record, and it can be seen that the local fluctuation BCDEFGH can be approximated with a type C_1 pulse with period $T_p^{C_1} \approx 0{\cdot}4$ s, and an approximate acceleration amplitude $a_p^{C_1} = \omega_p^{C_1} v_p^{C_1} = 0{\cdot}27g$, which is twice the value of the acceleration amplitude, $a_p^B = \omega_p^B v_p^B = 0{\cdot}14g$ of the long-duration type B pulse AIZ.

Consider now a set of geometrically similar blocks with slenderness α, and various sizes R, subjected to the El Centro, Array no. 5 acceleration shown in Fig. 16. As the base shakes, the blocks are subjected to the type C_1 pulse BCDEFGH. Within the limitations of the proposed approximate analysis, equation (45) indicates that any block with p such that

$$a_p^{C_1} \geqslant \alpha g\left(1 + \frac{1}{6}\frac{\omega_p^{C_1}}{p}\right) \tag{50}$$

will overturn due to the type C_1 pulse BCDEFGH. After rearranging terms, equation (50) gives

$$p \geqslant \frac{\omega_p^{C_1}}{6[(a_p^{C_1}/\alpha g) - 1]} \tag{51}$$

Accordingly, blocks which are small enough for inequality equation (51) to be satisfied will be overturned by the short-duration type C_1 pulse. Larger blocks will survive the type C_1 pulse BCDEFGH, and will be subjected to the long-duration type B pulse AIZ. According to equation (43), any block with p such that

$$a_p^B \geqslant \alpha g\left(1 + \frac{1}{4}\frac{\omega_p^B}{p}\right) \tag{52}$$

will overturn due to the type B pulse AIZ. Rearranging terms, inequality equation (52) gives

$$p > \frac{\omega_p^B}{4[(a_p^B/\alpha g) - 1]} \tag{53}$$

The substitution of

$$\omega_p^{C_1} = k\omega_p^B = k\omega_p,\ k > 1 \tag{54}$$

and

$$a_p^{C_1} = \mu a_p^B = \mu a_p,\ \mu > 1 \tag{55}$$

into equation (51) gives

$$\frac{\omega_p}{p} \leqslant 6\frac{[\mu(a_p/\alpha g) - 1]}{k} \tag{56}$$

Consequently, blocks which are small enough for inequality equation (56) to be satisfied will overturn due to the short-period type C_1 pulse, whereas, blocks of a size that satisfies

$$\frac{\omega_p}{p} \leqslant 4\left(\frac{a_p}{\alpha g} - 1\right) \tag{57}$$

will overturn due to the long-period type B pulse. The cut-off frequency is the intersection of the two lines defined by equations (56) and equation (57) when the equality sign is considered. For the El Centro, Array no. 5 station record, $k \approx 6$ and $\mu \approx 2$ and equations (56) and (57) intersect at $\omega_p/p \approx 2$. Fig. 17 shows that a block with ω_p/p less than 2 will overturn due to the short-duration pulse whereas blocks with $\omega_p/p > 2$ will overturn due to the long-duration type B pulse. This calculation indicates that the $0{\cdot}5$m $\times$ $1{\cdot}5$ m block with $p = 2{\cdot}157$ rad/s will overturn due to the short type C_1 pulse of the El Centro, Array no. 5 record, since $\omega_p = \omega_p^B = 2\pi/3{\cdot}2$ rad/s, and therefore $\omega_p/p = 0{\cdot}91$, which is less than 2. Fig. 18 shows the rocking response of the $0{\cdot}5$ m $\times$ $1{\cdot}5$ m block subjected to a near critical level of the El Centro, Array no. 5 motion. The block clearly overturns due to the presence of the short-duration pulse at approximately 123% level of the motion. Fig. 19(a) shows the minimum overturning acceleration spectrum of the El Centro,

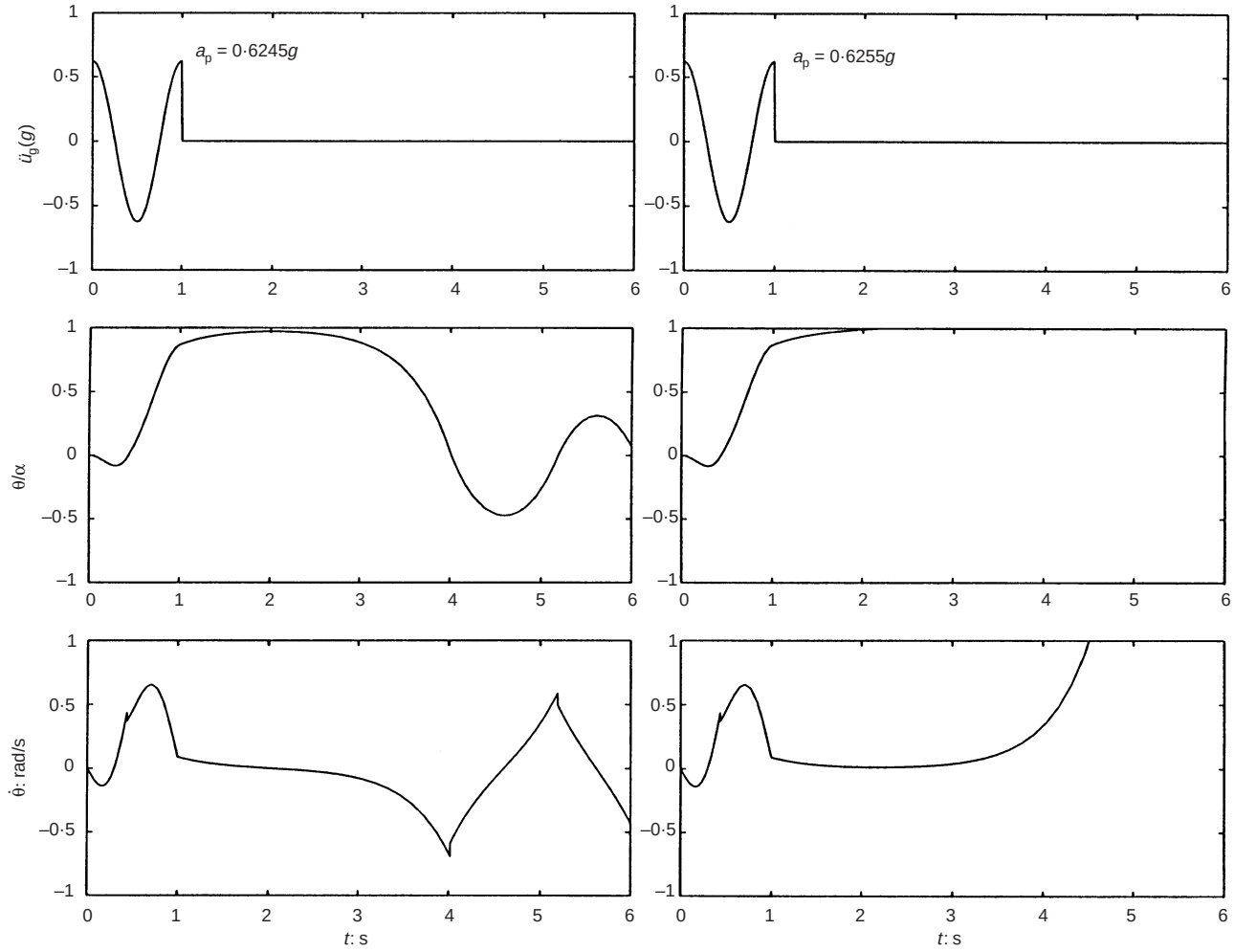

Fig. 11. Rotation and angular velocity time histories of a rigid block ($b = 0{\cdot}5$ m, $h = 1{\cdot}5$ m) subjected to a cycloidal pulse type B excitation. Left: no overturning. Right: overturning

Array no. 5 record as a function of ω_p/p, where $\omega_p = 2\pi/3{\cdot}2$ rad/s is the pulse frequency of the 3·2 s pulse. Indeed, the spectrum shows a distinct jump at $\omega_p/p \approx 2$. This is because, for values of $\omega_p/p < 2$, blocks overturn due to the presence of the short-period type C_1 pulse, whereas for values of $\omega_p/p > 2$, blocks overturn due to the long-duration type B pulse, as was predicted by Fig. 17. Fig. 19(b) plots the minimum overturning velocity spectrum of the El Centro, Array no. 5 record as a function of ω_p/p, where $\omega_p = 2\pi/3{\cdot}2$ rad/s. For values of $\omega_p/p > 2$, overturning of blocks occurs due to the 3·2 s type B pulse of the record, and the overturning velocity spectrum correlates better with the overturning velocity spectrum of a type B pulse, which is plotted with stars. For values of $\omega_p/p < 2$, overturning of blocks occurs due to the 0·4 s type C_1 pulse of the record. This explains the lack of correlation between the circles and the stars for $\omega_p/p < 2$.

The foregoing analysis shows that the overturning of rigid blocks under strong ground motions is a problem with several scales. Small blocks overturn as a result of small-duration pulses with high accelerations. Larger blocks overturn as a result of larger-duration pulses that might have smaller acceleration values. The example illustrated that blocks as big as a typical transformer ($p \approx 2$) overturn due to shorter pulses that have substantially shorter duration than the duration of the main pulse that generates most of the ground velocity and ground displacements. In contrast, larger objects such as the nuclear heat-exchange boilers with $p \approx 1$ (Hogan, 1989) will overturn due to the long-duration pulse.

The developed methodology is now used to estimate the level of the fault parallel component of the Lucerne Valley record shown in Fig. 4 that is needed to overturn the 0·5m × 1·5 m block ($p = 2{\cdot}157$, $\alpha = 0{\cdot}3217$). Fig. 20 zooms into the Lucerne Valley motion between 5 s and 15 s. On top of the 7·0 s forward pulse (AZ), one can distinguish a type C_2 pulse that crosses the AZ forward pulse at points BCDEFG. This type C_2 pulse has an approximate period of $T_p^{C_2} = 1{\cdot}14$ s and a velocity amplitude of $v_p^{C_2} = 0{\cdot}18$ m/s. The peak ground acceleration of the Lucerne Valley record occurs at $t \approx 11{\cdot}5$ s. This sharp spike is due to a short type B pulse with duration $T_p^B \approx 0{\cdot}2$ s. The characteristics of these three pulses, together with the values of their minimum overturning acceleration amplitudes a_{po} that were computed with equations (41), (43) and (45), are summarized in Table 1.

According to the approximate equations (41) and (45), the 0·5 m × 1·5 m block will overturn due to the long type A pulse when subjected to 15 times its level, and it will overturn due to the medium type C_2 pulse when subjected to 4·5 times its level. For the short type B pulse, the ratio $\omega_p/p = 14{\cdot}56$, and the approximate expression given by equation (43) is not applicable, since at high frequencies the minimum overturning acceleration spectrum increases non-linearly. Nevertheless, we adopt the conservative result of equation (43) for $\omega_p/p > 4$ as a crude improvement of West's formula. This conservative approximation indicates that the block will overturn due to the short type B pulse when subjected to 3·0 times its level. Fig. 21 shows that the 0·5 m × 1·5 m block overturns at a 2·74 level of the

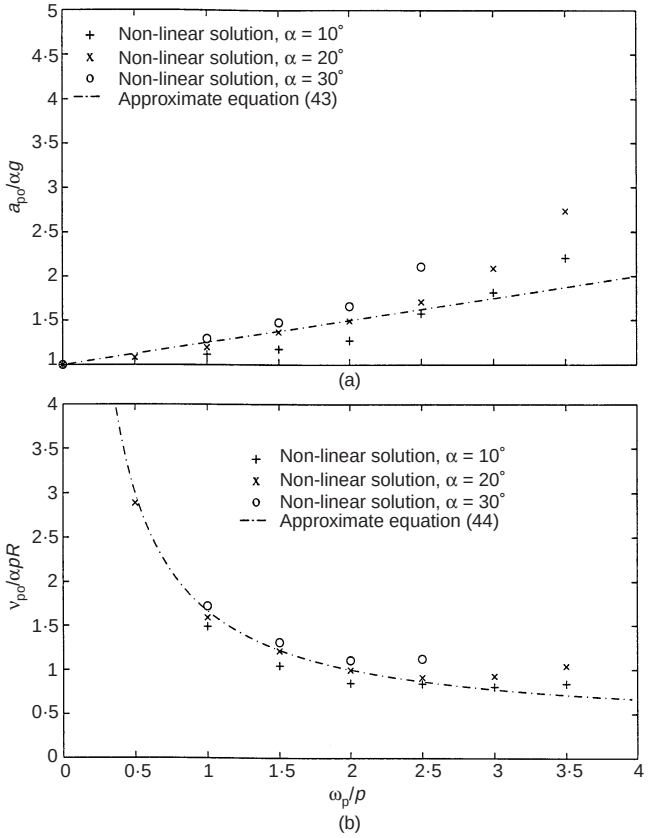

Fig. 12. Spectrum of the minimum acceleration amplitude (a) and velocity amplitude (b) of a type B pulse needed to overturn a free-standing block

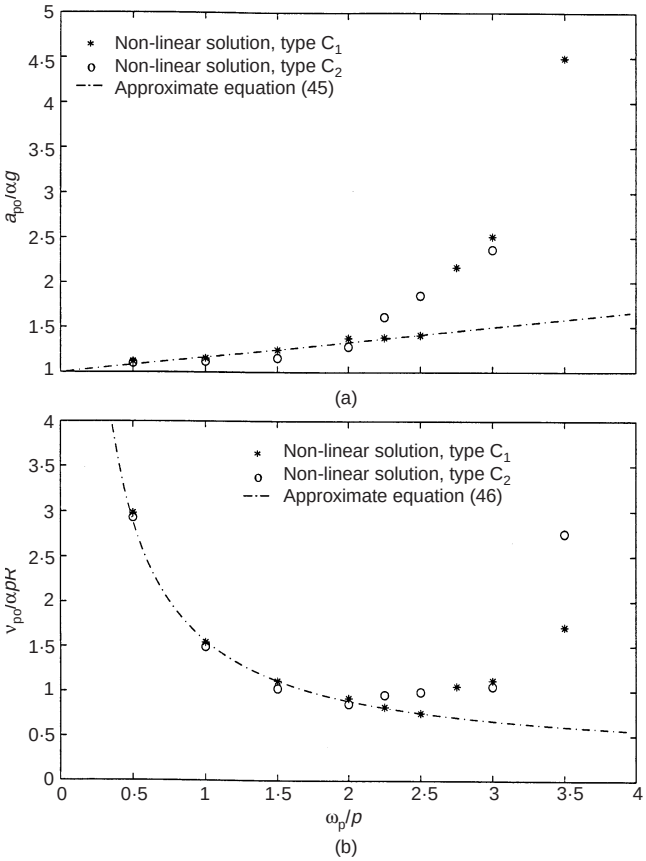

Fig. 13. Spectra of the minimum acceleration amplitude (a) and velocity amplitude (b) of a type C_1 pulse (stars) and a type C_2 pulse (circles) required to overturn a free-standing block

Lucerne Valley record, a value that is close to the 3·0 level that was computed with hand calculations.

Outline of proposed procedure

The outline of the proposed procedure to estimate the level of a given ground motion that is needed to overturn a free-standing rectangular block, with a given slenderness, α, and frequency parameter, p, is given below:

(*a*) Locate the time, in the record, of the peak ground acceleration, a_p. For instance, in the Lucerne Valley record, shown in Fig. 20, the maximum acceleration, a_p, occurs at approximately $t = 11{\cdot}5$ s.

(*b*) Zoom into the velocity record near the time of the peak ground acceleration, a_p, and identify the type and period, T_p, of the local pulse that results in the peak ground acceleration. Estimate the velocity amplitude, v_p, of the local pulse. The estimated values of T_p and v_p should satisfy $a_p \approx \omega_p v_p = 2\pi v_p / T_p$.

(*c*) Compute the minimum overturning acceleration $a_{po} = \alpha g[1 + \beta(\omega_p / p)]$ where $\beta = 1/6$ for type A or C_n pulses, and $\beta = 1/4$ for a type B pulse.

(*d*) Compute the ratio a_{po}/a_p. This ratio gives the approximate level of the ground motion that will overturn a block with slenderness α and frequency parameter p.

(*e*) If the velocity or displacement histories exhibit a distinguishable pulse other than the pulse that contains the peak ground acceleration, identify the velocity amplitude, v_p, and the duration, T_p, of this pulse. Then, compute the corresponding acceleration of this pulse as $a_p = 2\pi v_p / T_p = \omega_p v_p$.

(*f*) Compute the minimum overturning acceleration, a_{po}, of this pulse, as in step (*c*).

(*g*) Repeat step (*d*) using the value a_p estimated in step (*e*) and the value of a_{po} computed in step (*f*). If the ratio a_{po}/a_p that was computed in step (*g*) is larger than the ratio computed in step (*d*), the block overturns due to the short-duration pulse for the level of the ground motion computed in step (*d*). In contrast, if the ratio a_{po}/a_p computed in step (*g*) is smaller than the one computed in step (*d*), the block overturns due to the longer-duration pulse and for the level of the ground motion computed in step (*g*).

This study indicates that electrical transformers with approximate values of slenderness $\alpha \approx 20°$ and frequency parameter $p \approx 2$ rad/s, will most likely overturn due to the short duration pulse. Accordingly, only steps (*a*)–(*d*) are needed to estimate the level of the ground motion that will overturn a typical electrical transformer. Only very large objects, such as nuclear heat-exchange boilers, where the frequency parameter value is less than 1 ($p \leqslant 1$) may overturn due to the presence of the long-duration pulses. Thus, steps (*e*)–(*g*) should be included in the procedure.

CONCLUSIONS

The transient rocking response of a rigid block subjected to trigonometric pulses and near-source ground motion has been investigated in depth. First it was shown that the solution presented by Housner (1963) for the minimum acceleration amplitude of a half-sine pulse that is needed to overturn a rigid block is unconservative. In reality, under a half-sine pulse a block overturns during its free-vibration regime and not at the instant that the pulse expires. Within the limits of the linear approximation, the correct expression that yields the minimum acceleration required to overturn a block was derived.

Physically realizable trigonometric pulses have been intro-

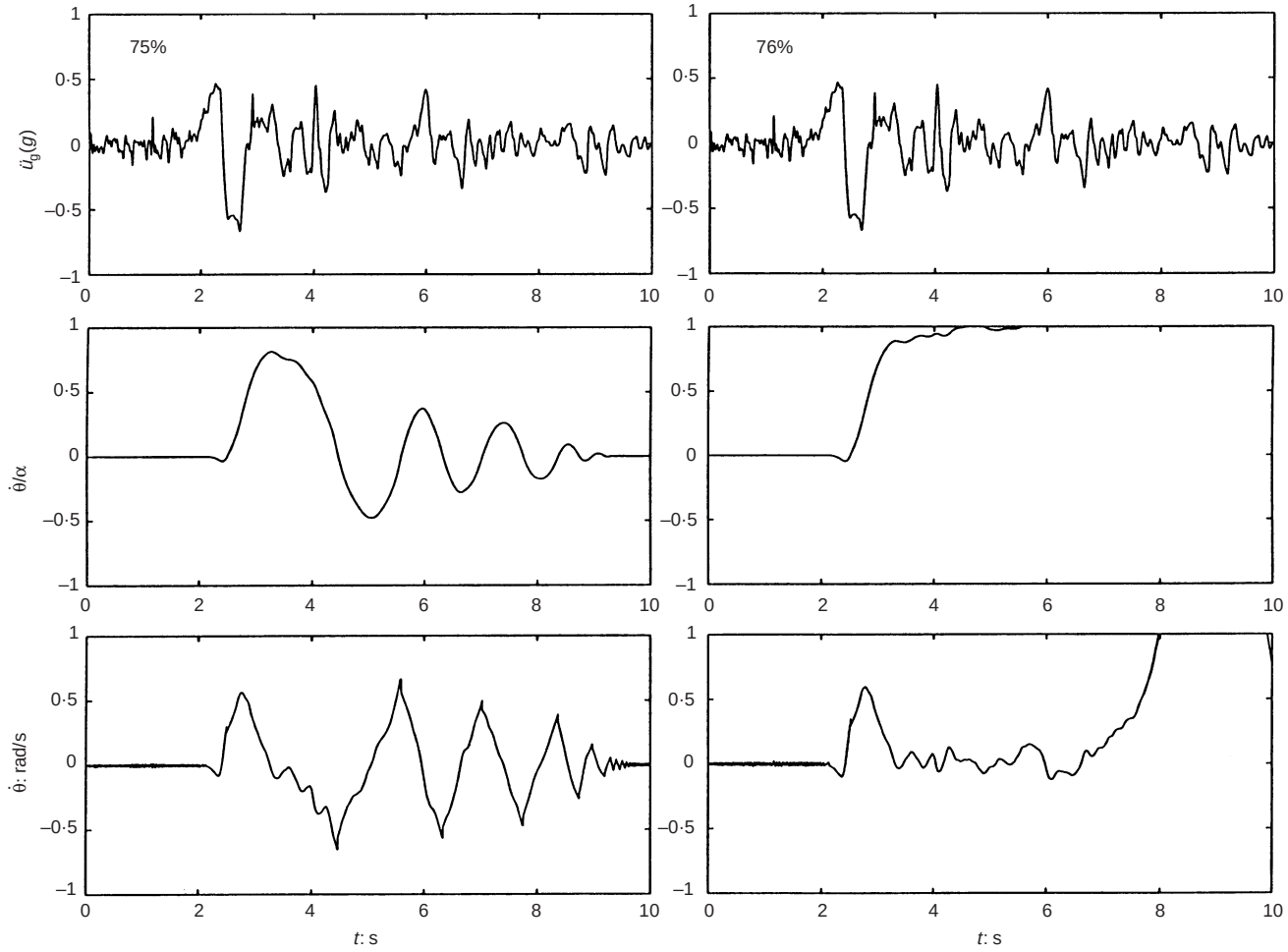

Fig. 14. Rotation and angular velocity response time histories of a rigid block ($b = 0{\cdot}5$ m, $h = 1{\cdot}5$ m) subjected to the fault normal Rinaldi station motion. Left: no overturning (75% acceleration level). Right: overturning (76% acceleration level)

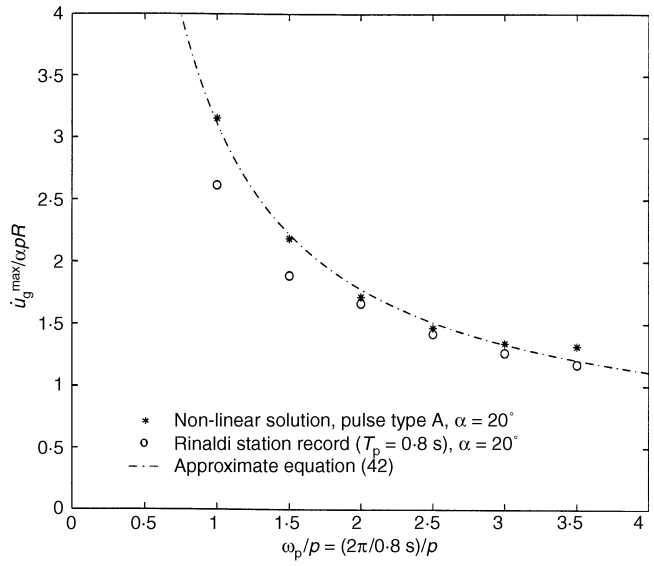

Fig. 15. Spectrum of the minimum velocity amplitude of the Rinaldi station motion (stars) and a pulse type A (circles), required to overturn a free-standing block

duced, and their resemblance to selected recorded near-source ground motions was illustrated. The overturning potential of forward pulses, forward-and-back pulses and pulses that result in displacement histories with one or two main cycles was examined. Under horizontal excitation, the three parameters that control overturning are the normalized pulse acceleration $a_p/\alpha g$, the frequency ratio ω_p/p and the slenderness α. It was found that at the low-frequency limit ($\omega_p/p < 3$), the normalized overturning acceleration amplitude of the pulse, $a_{po}/\alpha g$, is larger than one and increases linearly with ω_p/p. For values of $\omega_p/p > 3$, the normalized overturning acceleration amplitude increases non-linearly with ω_p/p, exhibiting a stiffening effect. Accordingly, the static solution (West's formula) is increasingly overconservative as ω_p/p increases.

The toppling of smaller blocks is more sensitive to the peak ground acceleration, whereas the toppling of larger blocks depends on the incremental ground velocity, which is the net increment of the ground velocity along a monotonic segment of its time histories. A simple method that involves hand calculations was developed to estimate the level of a recorded ground motion that is needed to overturn a given block. It was found that blocks as big as typical electric transformers ($p \approx 2$) overturn due to short-duration, high-acceleration pulses that often override the main long-duration pulse that generates most of the ground velocity and ground displacement recorded near the

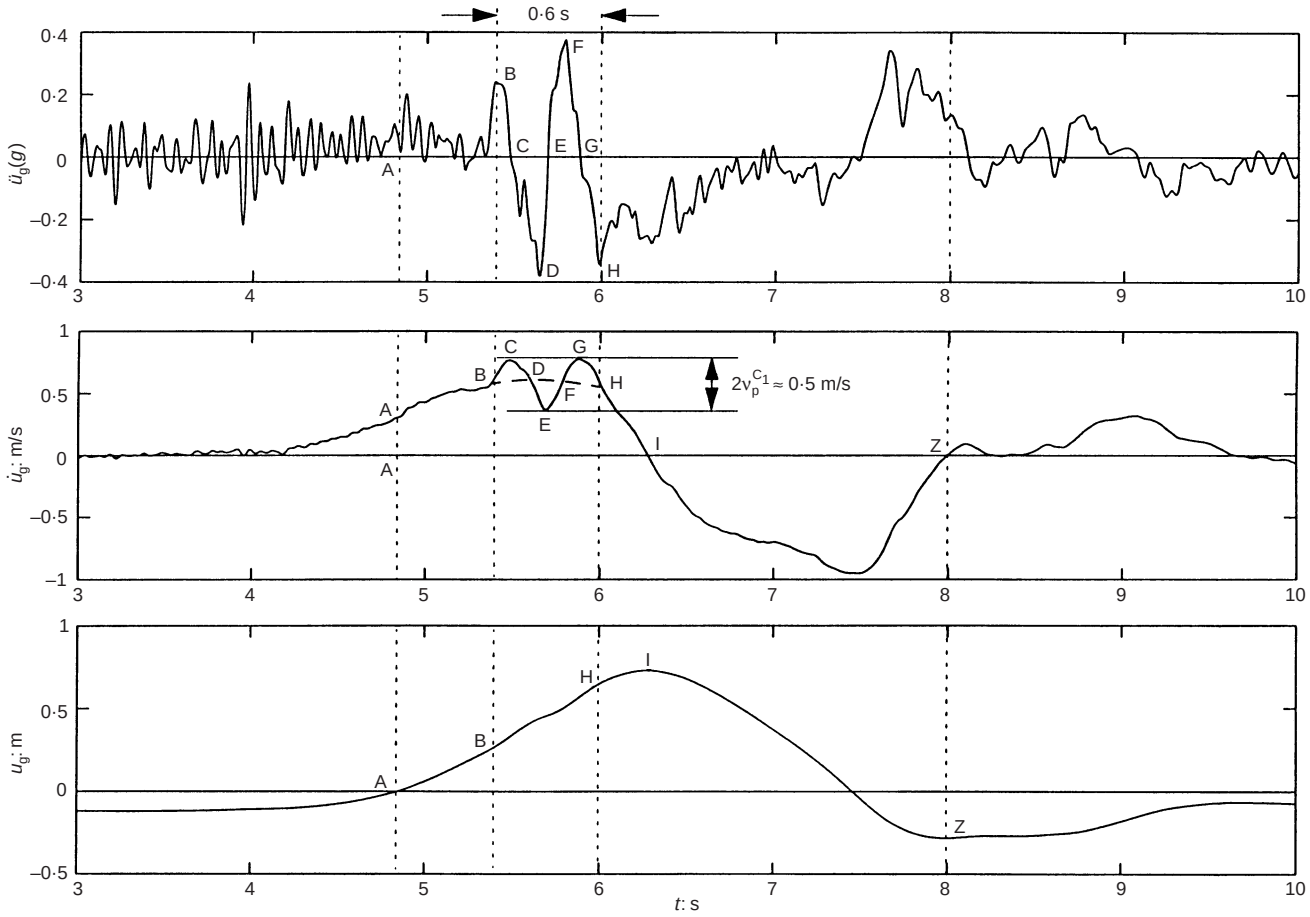

Fig. 16. Zoom into the acceleration, velocity and displacement histories recorded at the El Centro, Array no. 5 station, during the 15 October 1979 Imperial Valley, California earthquake

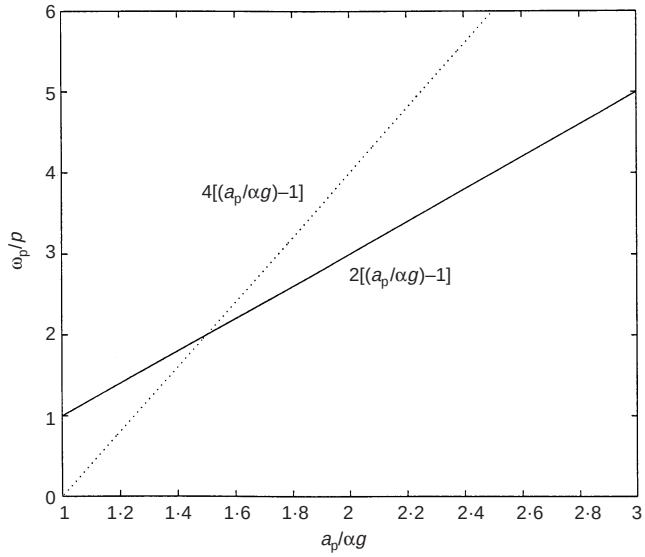

Fig. 17. Boundaries of the overturning region on the acceleration–frequency plane

source of strong ground motions. In contrast, larger objects such as nuclear heat-exchange boilers ($p \approx 1$) will overturn due to the long-duration pulse.

Under realistic conditions, the rocking response of a rigid block is affected by additional factors such as the vertical component of the ground acceleration and the additional energy loss due to plastic deformations at the pivot points. The effects of these factors are the subject of a future study. This study shows that the overturning potential of a recorded ground motion depends both on the duration and the acceleration level of its pulses.

The presented approximate method, although restricted to horizontal seismic excitations, elucidates the rocking response of rigid blocks, which is found to be quite ordered and predictable.

ACKNOWLEDGEMENT

This work was supported by the Pacific Gas and Electric Company, California. The authors are thankful to Professor James N. Brune (University of Nevada-Reno) for communicating to them the reference by Shi *et al.* (1996). The valuable input and comments of Dr Norm Abrahamson, Mr Eric Fujisaki,

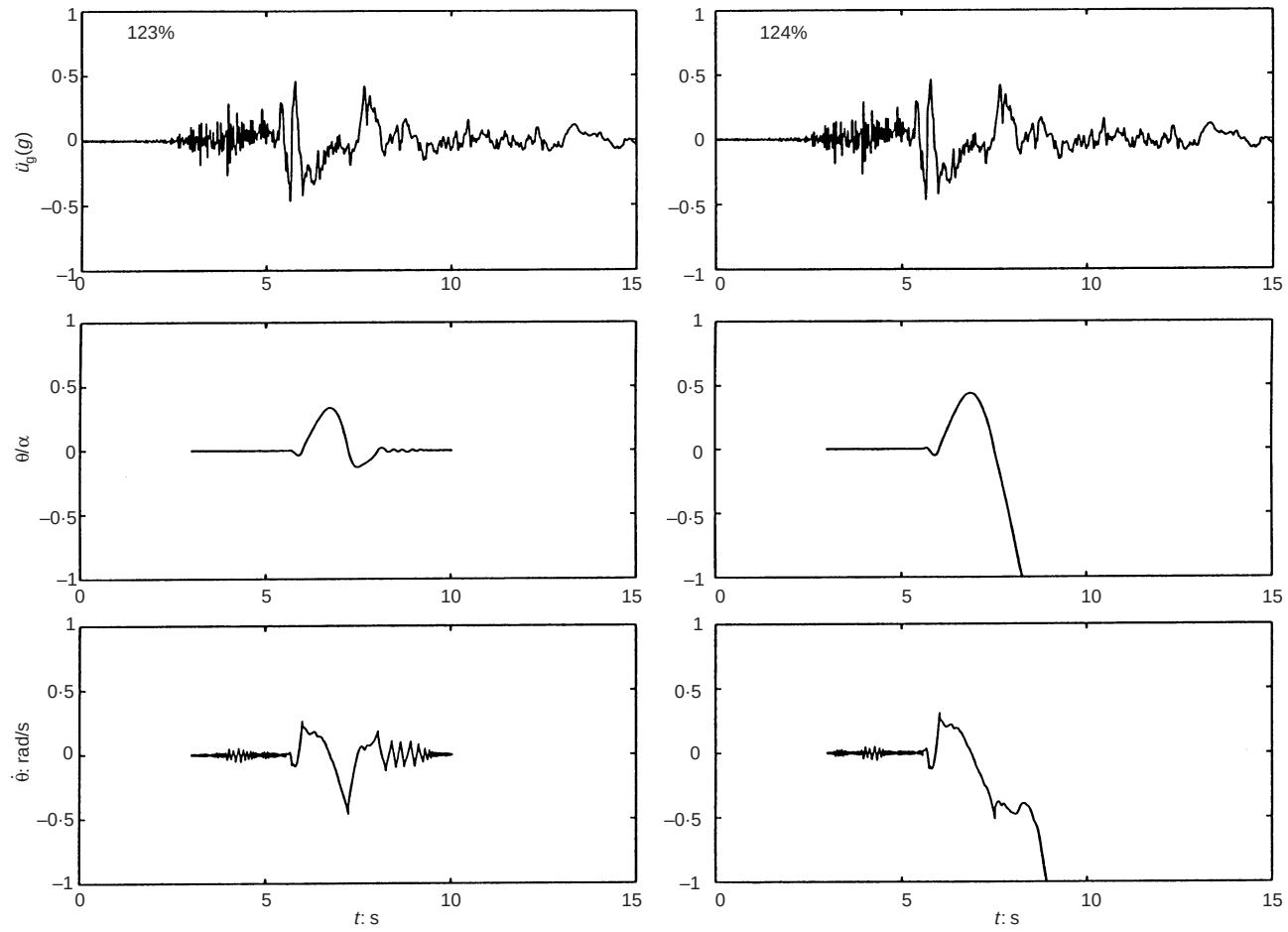

Fig. 18. Rotation and angular velocity response time histories of a rigid block ($b = 0{\cdot}5$ m, $h = 1{\cdot}5$ m) subjected to the El Centro, Array no. 5 motion. Left: no overturning (122% acceleration level). Right: overturning (123% acceleration level)

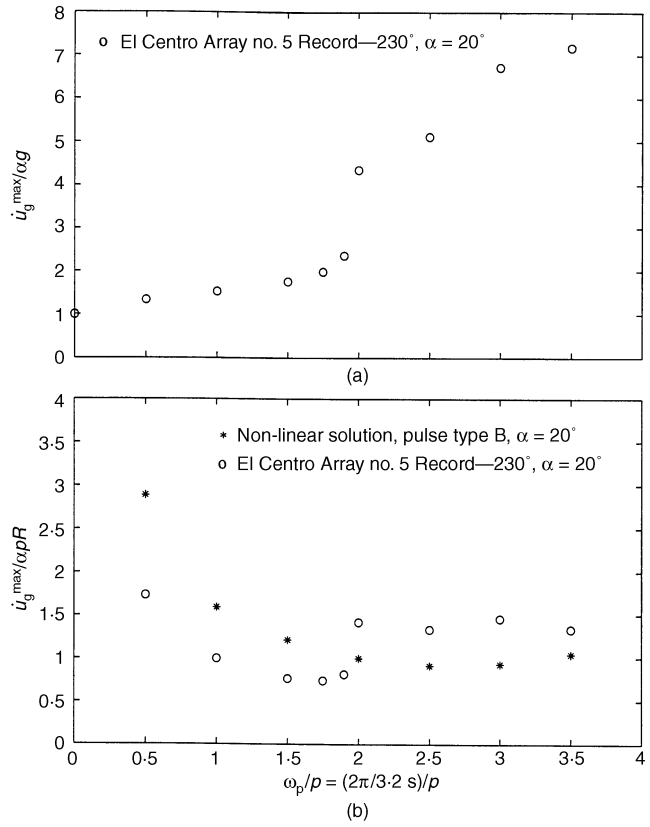

Fig. 19. Spectrum of the minimum peak acceleration (a) and velocity (b) of the El Centro, Array no. 5 motion needed to overturn a free-standing block. The sudden jump near $\omega_p/p = 2$ indicates that smaller blocks ($\omega_p/p < 2$) overturn due to the presence of a pulse that is different from the pulse that overturns the larger blocks $\omega_p/p \geqslant 2$

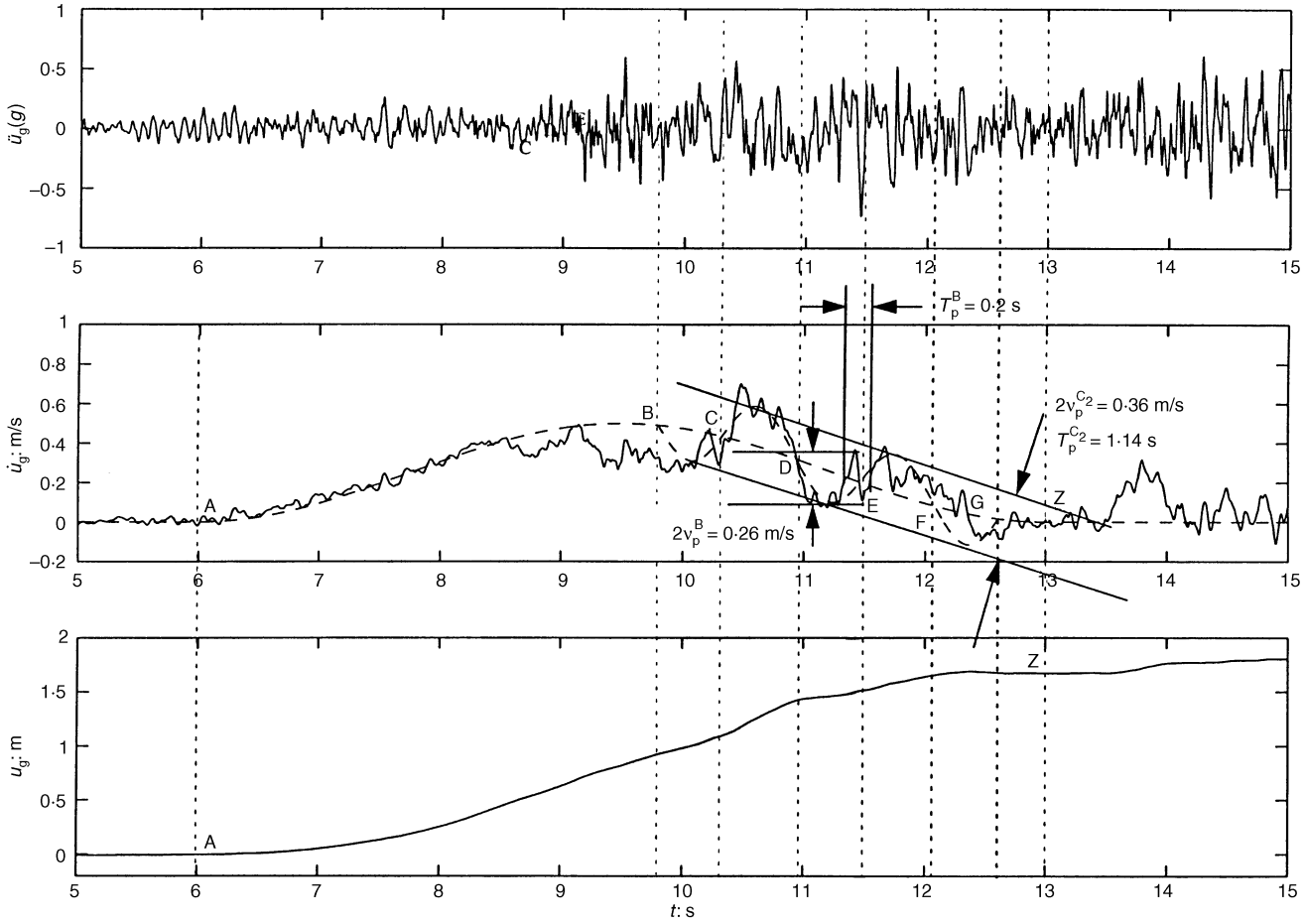

Fig. 20. Zoom into the acceleration, velocity and displacement histories recorded at the Lucerne Valley station during the 28 June 1992 Landers, California earthquake

Table 1. Characteristics of three distinct pulses of the Lucerne Valley record and their levels needed to overturn the 0·5 m × 1·5 m block ($p = 2{\cdot}157$, $\alpha = 0{\cdot}3217$)

Pulse type/ pulse characteristics	Long pulse type A	Medium pulse type C_2	Short pulse type B
v_p: m/s	0·50	0·18	0·133
T_p: s	7·0	1·14	0·20
ω_p: rad/s	0·90	5·51	31·41
a_p: g	0·032	0·101	0·500
ω_p/p	0·417	2·555	14·56
$a_p/\alpha g$	0·071	0·314	1·55
$a_{po}/\alpha g$	$1+\frac{1}{6}\frac{\omega_p}{p} = 1{\cdot}07$	$1+\frac{1}{6}\frac{\omega_p}{p} = 1{\cdot}426$	$1+\frac{1}{4}\frac{\omega_p}{p} = 4{\cdot}64$
a_{po}/a_p	15	4·5	3·00

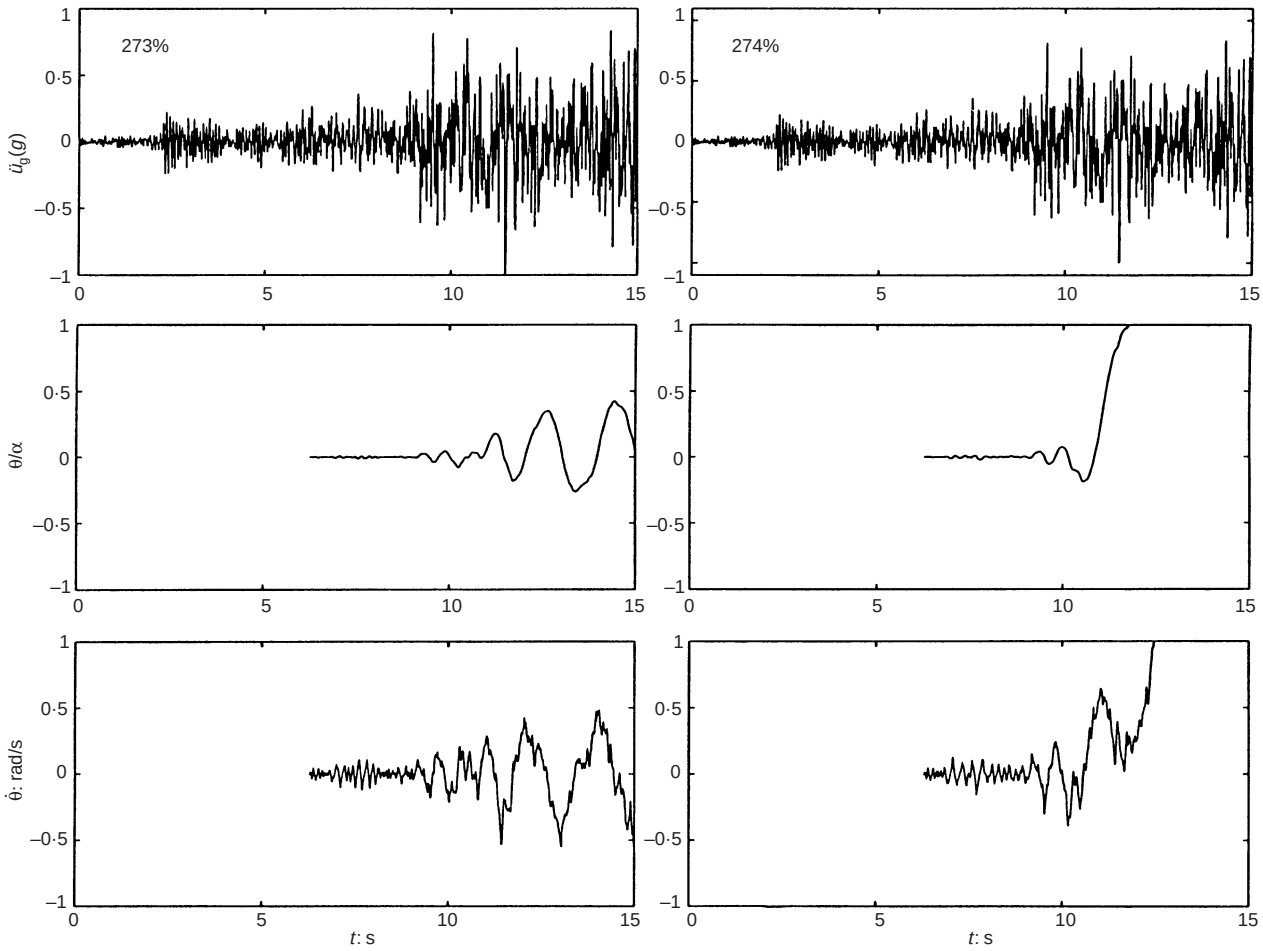

Fig. 21. Rotation and angular velocity histories of a rigid block ($b = 0{\cdot}5$ m, $h = 1{\cdot}5$ m) subjected to the motion recorded at the Lucerne Valley station. Left: no overturning (273% acceleration level). Right: overturning (274% acceleration level)

Mr Henry Ho and the anonymous referee and assessor are greatly appreciated.

NOTATION

A_i	integration constant
a_p	acceleration amplitude of trigonometric pulse
a_{po}	minimum amplitude of acceleration pulse needed to create overturning
$2b$	width of rigid block
$\{f(t)\}$	time derivative vector
g	acceleration of gravity
$2h$	height of rigid block
I_0	moment of inertia of rigid block about point O
k	scalar factor
m	mass of rigid block
n	number of cycles
$p = \sqrt{\frac{g}{4R}}$	frequency parameter
R	distance between the centre of gravity of the rigid block and any of its corners
r	coefficient of restitution
sgn[ ]	signum function
t	time
t_0	time when trigonometric pulse initiates
$T_p = \frac{2\pi}{\omega_p}$	period of trigonometric pulse
$\ddot{u}_g$	ground acceleration
$\dot{u}_g$	ground velocity
u_g	ground displacement
v_p	velocity amplitude of trigonometric pulse
v_{po}	minimum amplitude of velocity pulse needed to create overturning
$\{y(t)\}$	state vector
$\alpha = \tan^{-1}(b/h)$	slenderness of rigid block
β	scalar coefficient
θ	angle of rotation of rigid block
$\dot{\theta}$	angular velocity of rigid block
μ	scalar factor
$\tau = t - t_0$	time variable in trigonometric pulse
φ	phase angle
$\psi = \sin^{-1}(\alpha g/a_p)$	phase angle when rocking initiates
$\omega_p = \frac{2\pi}{T_p}$	circular frequency of trigonometric pulse

REFERENCES

Anderson, J. C. & Bertero, V. (1986). Uncertainties in establishing design earthquakes. *J. Struct. Engng*, ASCE **113**, 1709–1724.

Aslam, M., Godden, W. G. & Scalise, D. T. (1980). Earthquake rocking response of rigid bodies, *J. Engng Mech. Div.* ASCE **106**, 377–392.

Campillo, M., Gariel, J. C., Aki, K. & Sanchez-Sesma, F. J. (1989). Destructive strong ground motion in Mexico City: source, path and site effects during the great 1985 Michoagan earthquake, *Bull. Seism. Soc. Am.* **79**, No 6, 1718–1735.

Hogan, S. J. (1989). On the dynamics of rigid-block motion under harmonic forcing. *Proc. R. Soc. Lond.*, **A425**, 441–476.

Hogan, S. J. (1990). The many steady state responses of a rigid block under harmonic forcing. *Earthquake Engng Struct. Dynamics* **19**, 1057–1071.

Housner, G. W. (1963). The behaviour of inverted pendulum structures during earthquakes. *Bull. Seism. Soc. Am.* **53**, 404–417.

Iwan, W. D. & Chen, X. D. (1994). Important near-field ground motion

data from the Landers earthquake *Proc. 10th Eur. Conf. Earthquake Engng,* Balkema, Rotterdam, **1**, 229–234.

Jacobsen, L. S. & Ayre, R. S. (1958) *Engineering vibrations*. New York: McGraw-Hill.

Makris, N. (1997). Rigidity–plasticity–viscosity: can electrorheological dampers protect base-isolated structures from near-source ground motions? *Earthquake Engng Struct. Dynamics* **26**, 571–591.

MATLAB (1992). *High-performance numeric computation and visualization software*. Natick, MA: The MathWorks.

Milne, J. (1885). Seismic experiments, *Trans. Seism. Soc. Japan* **8**, 1–82.

Pompei, A., Scalia, A. & Sumbatyan, M. A. (1998). Dynamics of rigid block due to horizontal ground motion, **124**, 713–717.

Scalia, A. & Sumbatyan, M. A. (1996). Slide rotation of rigid bodies subjected to a horizontal ground motion. *Earthquake Engng Struct. Dynamics* **25**, 1139–1149.

Shi, B., Anooshehpoor, A., Zeng, Y. & Brune, J. N. (1996). Rocking and overturning of precariously balanced rocks by earthquake. *Bull. Seism. Soc. Am.* **86**, No. 5, 1364–1371.

Spanos, P. D. & Koh, A. S. (1984). Rocking of rigid blocks due to harmonic shaking, *J. Engng Mech. Div. ASCE* **110**, 1627–1642.

Tso, W. K. & Wong, C. M. (1989a). Steady state rocking response of rigid blocks. Part 1: Analysis. *Earthquake Engng Struct. Dynamics* **18**, 89–106.

Tso, W. K. & Wong, C. M. (1989b). Steady state rocking response of rigid blocks. Part 2: Experiment. *Earthquake Engng Struct. Dynamics* **18**, 107–120.

Yim, C. K., Chopra, A. K. & Penzien, J. (1980). Rocking response of rigid blocks to earthquakes. *Earthquake Engng Struct. Dynamics* **8**, 565–587.